A volatility basis set model for summertime secondary organic aerosols over the eastern United States in 2006

R. Ahmadov,[1,2] S. A. McKeen,[1,2] A. L. Robinson,[3] R. Bahreini,[1,2] A. M. Middlebrook,[1] J. A. de Gouw,[1,2] J. Meagher,[1] E.-Y. Hsie,[1,2] E. Edgerton,[4] S. Shaw,[5] and M. Trainer[1]

Received 2 September 2011; revised 4 January 2012; accepted 4 January 2012; published 16 March 2012.

[1] A new secondary organic aerosol (SOA) parameterization based on the volatility basis set is implemented in a regional air quality model WRF-CHEM. Full meteorological and chemistry simulations are carried out for the United States for August–September 2006. Predicted organic aerosol (OA) concentrations are compared against surface measurements made by several networks and aircraft data from the TexAQS-2006 field campaign. Elemental carbon simulations are also evaluated in order to evaluate the model's ability to capture their emissions, transport, and removal. Certain measurement limitations, such as daily averaged OA concentrations, impose some difficulties on the model evaluation, and hourly averaged OA measurements provide more informative constraints compared to daily concentrations. The updated model demonstrates a significant improvement in simulating the OA concentrations compared to the standard WRF-CHEM, which predicts very little SOA. The improvement in organic carbon (OC) predictions is noticeable in correlations and model bias. The correlations of OC exceed that of the persistence forecasts for hourly concentrations in the southeast United States during daytime. The updated traditional SOA yields still lead to an underestimation of observed OA, while addition of the multigenerational volatile organic compound (VOC) oxidation drastically improves model performance. However, several key uncertainties remain in SOA formation and loss mechanisms, which are characterized through several perturbation simulations. Dry deposition of VOC oxidation products is an important factor in the atmospheric SOA budget. The combination of the biogenic VOC emissions, updated SOA yields, and aging mechanism result in biogenic SOA being the dominant OA component for much of the nonurban United States.

Citation: Ahmadov, R., et al. (2012), A volatility basis set model for summertime secondary organic aerosols over the eastern United States in 2006, *J. Geophys. Res.*, *117*, D06301, doi:10.1029/2011JD016831.

1. Introduction

[2] Atmospheric aerosols have a strong impact on climate, air quality and visibility. Organic matter makes up the significant fraction of the submicron aerosol composition [*Zhang et al.*, 2007]. OA consists of thousands of very complex molecules, thus making it very hard to identify their sources and transformation processes in the atmosphere, and their effects on human health and climate [*Hallquist et al.*, 2009]. OA is emitted directly to the atmosphere by sources, such as diesel engines, cooking and fires. In addition a significant portion of OA is formed in the atmosphere by the photochemical oxidation of VOCs. SOA has been detected in the atmosphere and laboratory experiments as oxidized OA with a wide range of volatility, hygroscopicity and reactivity [*Jimenez et al.*, 2009]. Since the formation and evolution of the SOA species are quite complicated, it is challenging to represent those processes in air quality and climate models.

[3] Atmospheric chemistry models have traditionally underpredicted observed OA concentrations, possibly due to missing key precursors and processes involved in SOA production and evolution, especially in summer months [*Bhave et al.*, 2007; *Carlton et al.*, 2010; *Yu et al.*, 2007]. The rapid and significant formation of SOA downwind of the concentrated VOC sources is well established from a number of field campaigns [*de Gouw et al.*, 2008; *Volkamer et al.*, 2006]. An evaluation study based on a field campaign over East Texas in September of 2006 revealed that the rapid SOA formation occurring within 1–3 h downwind of Dallas and Houston is not captured by several regional air quality forecast models [*McKeen et al.*, 2009]. *Heald et al.* [2005] showed that global atmospheric chemistry models systematically

[1]Chemical Sciences Division, Earth System Research Laboratory, NOAA, Boulder, Colorado, USA.
[2]Cooperative Institute for Research in Environmental Sciences, University of Colorado at Boulder, Boulder, Colorado, USA.
[3]Center for Atmospheric Particle Studies, Carnegie Mellon University, Pittsburgh, Pennsylvania, USA.
[4]Atmospheric Research and Analysis, Inc., Cary, North Carolina, USA.
[5]Electric Power Research Institute, Palo Alto, California, USA.

Copyright 2012 by the American Geophysical Union.
0148-0227/12/2011JD016831

underpredict the OA concentrations in the free troposphere. These systematic low biases in OA predictions by atmospheric chemistry models have led the aerosol research community to an intensive search for additional SOA precursors and formation mechanisms.

[4] In recent years significant progress has been achieved in modeling OA mass concentrations in the atmosphere. The progress is due to several key improvements in the understanding and quantification of different SOA formation mechanisms. First of all, recent SOA mass yields obtained from smog chamber measurements proved to be much higher than previously reported [*Hildebrandt et al.*, 2009; *Ng et al.*, 2007]. Furthermore, the model treatment of SOA formation from some abundant precursors, such as isoprene, has advanced greatly [*Carlton et al.*, 2009; *Carlton et al.*, 2010]. The possible formation of a considerable amount of SOA within clouds has been reported [*Hallquist et al.*, 2009], and in-cloud SOA generation pathways have been implemented in several atmospheric chemistry models [*Ervens et al.*, 2008; *Fu et al.*, 2009].

[5] Another significant SOA source missing in traditional aerosol models was proposed by *Robinson et al.* [2007]. Based on laboratory studies, this work demonstrated three important features of SOA formation from combustion sources: (1) "primary" organic aerosol (POA) depends strongly on the partitioning of semivolatile organic compounds; (2) a large pool of organic compounds with intermediate volatilities is missing from traditional emission inventories; and (3) the photochemical aging of compounds with higher volatility to compounds with lower volatility can be a significant source of SOA. Conceptually, these results are best explained by treating the gas/aerosol system within a spectrum of volatilities using saturation vapor concentration as the surrogate for volatility [*Donahue et al.*, 2006]. For modeling applications this volatility spectrum is divided into a manageable number of bins, or basis sets, where each bin represents a factor of 10 increase in saturation vapor concentration from the previous bin. This approach allows lumping organic mass to different volatility bins, circumvents the detailed kinetics leading to SOA from various precursors, and makes it easier to describe the effects of oxidation (aging) processes of complex mixtures on gas/aerosol partitioning within atmospheric models.

[6] Different variations of the VBS approach and proposed SOA precursors have been included in a number of regional and global modeling frameworks [*Farina et al.*, 2010; *Hodzic et al.*, 2010; *Lane et al.*, 2008a; *Murphy and Pandis*, 2009; *Pye and Seinfeld*, 2010; *Shrivastava et al.*, 2011; *Tsimpidi et al.*, 2010]. These modeling studies significantly reduced the gap between the simulations and the observations of OA concentrations. In addition, hydrocarbon-like OA (HOA) and oxygenated OA (OOA) fractions of the measured OA mass (HOA:OOA) have been compared with the models assuming they are primary and secondary components of OA, respectively. Some authors [e.g., *Hodzic et al.*, 2010; *Shrivastava et al.*, 2011] have also evaluated oxygen to carbon ratios as an additional constraint for the SOA mechanisms.

[7] Despite these achievements, different model results reveal significant differences in the SOA parameterizations. Three model studies of SOA in Mexico City during the 2006 MILAGRO study illustrate this point. According to *Tsimpidi et al.* [2010], the major improvement in SOA simulations is due to aging of the organic condensable vapors (OCV) formed during VOC oxidation over Mexico City. *Hodzic et al.* [2010] compared and evaluated two recently proposed SOA mechanisms based on VBS (but without OCV aging) within one modeling framework, and concluded that semivolatile and intermediate precursor emissions are the major missing SOA source in megacity environments. *Shrivastava et al.* [2011] showed that the inclusion of nontraditional SOA precursor emissions improves OA predictions over Mexico city, however overpredicts downwind of the city. Their simulations underpredicted the oxygen to carbon ratios downwind as compared to measurements, suggesting a need to further improve chemistry parameterizations of SOA formation.

[8] An essential question related to SOA modeling arises: Are the models getting the right answer for the right reasons? It should be noted that the new SOA mechanisms are usually implemented in atmospheric models with different volatility bins, oxidation/aging reactions (and their rates), and emissions of nontraditional SOA precursors. Other uncertainties include different mass yields used for traditional SOA formation pathways, their multigenerational aging, and oligomerization. Undoubtedly, common uncertainties in atmospheric chemistry models related to the emissions from anthropogenic and biogenic sources, gas and aerosol chemistry mechanisms, removal processes, boundary conditions for chemical species and meteorological simulations further contribute to the disparities between the models. Some of these uncertainties were investigated by *Murphy and Pandis* [2010] and *Farina et al.* [2010] by perturbing some parameters and processes driving the atmospheric SOA. The oxidized OCVs are soluble, thus becoming more susceptible to dry and wet removal processes, which imposes a large uncertainty in SOA simulations since the removal of the OCVs is not well constrained by observations. *Bessagnet et al.* [2010] found that neglecting dry deposition of these species may lead to overestimations of SOA concentrations by as much as 50%.

[9] Another remaining question in atmospheric SOA is the quantification of the role of anthropogenic versus biogenic sources on atmospheric SOA formation. *Weber et al.* [2007] found that fine particle organic compounds in water spatially correlate with vehicle emission tracers over some urban regions in the United States. In contrast, their radiocarbon analysis showed that ≈70–80% of carbon in the samples was modern, suggesting a strong contribution to SOA formation from biogenic sources. *de Gouw et al.* [2009] used carbonyl sulfide as a tracer for biogenic emissions but found a poor correlation with water soluble organic carbon. *Kleindienst et al.* [2007] examined the contributions of SOA formed by different VOCs at a southeastern United States site during 2003 using an organic tracer-based method. The analysis found significant SOA production from biogenic VOCs such as isoprene and terpenes during summer months, when observed OC at the station was high. *Schichtel et al.* [2008] analyzed fossil and contemporary carbon fractions of fine particles in a number of locations during winter and summer. Similar to *Weber at al.* [2007], the analysis showed that, on average, modern carbon composed about half of the carbon at the urban, ∼70–97% at near-urban, and 82–100% at remote sites throughout the United States. *Hoyle et al.*

Table 1. Acronyms Used in the Text

Acronyms	Description
PM2.5	Particulate matter with diameter less than 2.5 mm
OA	Organic aerosols (total mass including oxygen and other elements)
OCV	Organic condensable vapor (VOC oxidation product, which condenses on particles)
OC	Organic carbon (only carbon mass)
EC	Elemental carbon
VOC	Volatile organic compound
POA	Primary organic aerosols
SOA	Secondary organic aerosols
ASOA	Anthropogenic secondary organic aerosols
BSOA	Biogenic secondary organic aerosols
HOA	Hydrocarbon-like organic aerosol
OOA	Oxygenated organic aerosol
PBL	Planetary boundary layer
VBS	Volatility basis set
AMS	Aerodyne aerosol mass spectrometer
WRF-CHEM	Weather Research and Forecasting Model Coupled to Chemistry
RACM	Regional Atmospheric Chemistry Mechanism
MB	Mean bias
MMO	Median of model over observation
IMPROVE	Interagency Monitoring of Protected Visual Environments
STN	Speciation Trends Network
SEARCH	Southeastern Aerosol Research and Characterization
LST	Local standard time

[2011] give a broad overview of different observations and methods that study anthropogenic and biogenic OC components, and discusses the mechanisms through which anthropogenic emissions may affect biogenic SOA formation.

[10] In this study we use the WRF-CHEM model for the following purposes: (1) to implement a new SOA parameterization with updated yields, the multigenerational oxidation mechanism for VOCs and the VBS mechanism within the WRF-CHEM model framework in order to improve OA predictions; (2) to perform sensitivity analysis to address key uncertainties affecting the SOA predictions; (3) to evaluate the WRF-CHEM sensitivity runs for the U.S. region using the measurements from the surface particulate matter ($PM_{2.5}$) composition networks and aircraft measurements made over Houston and Dallas cities and their downwind; and (4) to quantify the contribution of different emissions categories (primary OA, anthropogenic VOCs and biogenic VOCs) to OA concentrations.

[11] The WRF-CHEM model is a fully coupled meteorology-chemistry model suitable for applications ranging from regional air quality to global atmospheric chemistry modeling. The model allows a user to select between numerous physics and chemistry options, different dynamics and other settings. The meteorological core of the model, WRF (http://www.wrf-model.org), simulates various meteorological processes such as advection, vertical mixing, convection, land-atmosphere interactions, microphysics and radiation.

[12] The traditional WRF-CHEM model [*Grell et al.*, 2005] uses the SORGAM parameterization [*Schell et al.*, 2001], which is based on a two-product approach [*Odum et al.*, 1996] of VOC oxidation with older SOA yield estimates. This parameterization predicts very little SOA formation, with OA predictions dominated by model POA emissions. It also substantially underestimates OA concentrations in rural areas, especially within urban plumes [*McKeen et al.*, 2007]. In this study WRF-CHEM is updated with the VBS approach as described in section 2. The formalism is confined to traditional SOA precursors taking into account multigenerational oxidation.

[13] The paper consists of the following sections: 2, Model and Surface Observations; 2.1, WRF-CHEM Settings and the SOA Parameterization; 2.2, Different Model Scenarios; 2.3, Surface Observations; 3, Discussion of the Results; 3.1, Evaluation of the Model Using the Surface Data: Hourly Concentrations; 3.2, Evaluation of the Model Using the Surface Data: Daily Concentrations; 3.3, Evaluation of OA Aloft: TexAQS-2006 Field Campaign; and 4, Conclusions. Table 1 lists all the acronyms used in the paper.

2. Model and Surface Observations

2.1. WRF-CHEM Settings and the SOA Parameterization

[14] WRF-CHEM was configured to simulate atmospheric conditions over the continental United States (Figure 1). The model was run with full tropospheric chemistry for the time period of August–September 2006. The main settings of the model configuration are given in Table 2. No feedback mechanism between the chemistry and the meteorological simulations is included in the model. Numerous WRF-CHEM runs were undertaken to identify the optimal physics and chemistry options for our domain. In this section we discuss the gas chemistry and aerosol configurations used in our model runs.

[15] The simulations were performed with the Regional Atmospheric Chemistry Mechanism (RACM). Table 3 shows the list of primary VOC species included in the mechanism that contribute to SOA formation. The RACM chemistry mechanism has a full range of photolysis and gas phase reactions, inorganic and organic species to perform air pollution studies [*Stockwell et al.*, 1997] and we used the updated version (RACM_ESRL option) in WRF-CHEM. Reaction rates with hydroxyl radical for the VOCs are presented in Table 3 as well.

[16] Anthropogenic emissions are based on the U.S. EPA National Emission Inventory version 2005 (NEI2005) [*U.S. Environmental Protection Agency*, 2010]. Processing for the four major components; point, mobile on-road, mobile nonroad, and area, were done according to EPA recommendations with emissions data available through the U.S. EPA as of October of 2008. The gridded (4 km resolution) and point source hourly emission files used in this study are available electronically at ftp://aftp.fsl.noaa.gov/divisions/taq/emissions_data_2005/. Specific details of the anthropogenic inventory are available in the readme.txt file that comes with the emissions. Year-specific wildfire and prescribed burning sources are missing from the inventory, though other fire sources, such as agricultural burning, are included as area sources. Biogenic emissions are based on the Biogenic Emissions Inventory System version 3.14 (BEIS 3.14), which is an update to BEIS version 3.12 (U.S.

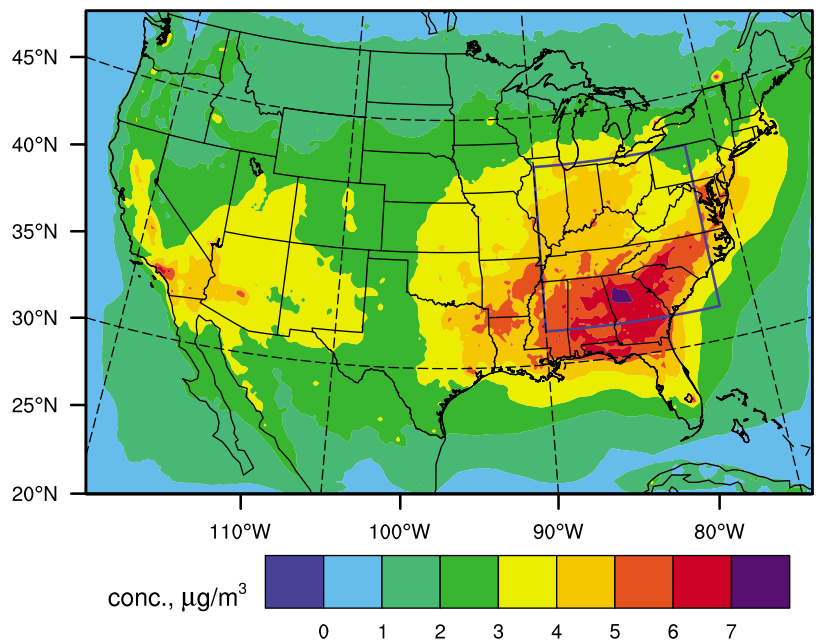

Figure 1. Entire modeling domain with 20 km resolution and OA concentrations near surface averaged from 4 August to 28 September 2006. OA from the HR6 sensitivity run is shown.

EPA, http://www.epa.gov/ttn/chief/emch/biogenic/) and BEIS version 3.13 [*Schwede et al.*, 2005] to include emissions of sesquiterpenes. The total U.S. anthropogenic and biogenic emissions of the SOA precursors east of 104°W longitude used in the model can be found in Table 3.

[17] For particle parameterizations the Modal Aerosol Dynamics for Europe (MADE) [*Ackermann et al.*, 1998] scheme is selected. MADE is a computationally efficient module that deploys two overlapping lognormal modes to simulate aerosol size distribution. We completely updated the SOA module within WRF-CHEM by introducing a four-bin volatility basis set with the updated SOA yields based on the smog chamber studies (Table 4) [*Murphy and Pandis*, 2009]. The Clausius-Clapeyron equation is used to calculate the saturation concentrations for different temperatures. Pseudoideal partitioning theory [*Pankow*, 1994] is used to partition between the gas phase OCVs and particulate phase OA for each volatility bin, n:

$$c_n^{aer} = \frac{c_n^{tot}}{\left(1 + c_n^*/M\right)} \tag{1}$$

c_n^{aer} is organic aerosol concentration at a given volatility bin n, c_n^{tot} is sum of OCV and SOA mass concentrations for bin n, c_n^* is saturation concentration for bin n, M is total OA mass comprising POA and SOA. Therefore, SOA is assumed to form a pseudoideal solution with all organic aerosol

Table 2. Settings and Parameterizations Used for the WRF-CHEM3.1.1 Model[a]

Category	Selected Options and Parameters
Land surface	Noah Land Surface Model
PBL scheme	Mellor-Yamada Nakanishi and Niino
Microphysics	Purdue Lin scheme
Cumulus	Grell 3-D ensemble
Shortwave and longwave radiation	RRTMG shortwave and longwave
Global meteorological fields	Global Forecast System, 6 hourly
Gas chemistry	RACM_ESRL
Aerosol	MADE
Aerosol feedback	No
Photolysis	Madronich
Anthropogenic emissions	NEI2005
Biogenic emissions	BEIS 3.14
Horizontal resolution	60 and 20 km
Number of vertical layers	40

[a]Available at http://www.wrf-model.org.

Table 3. VOC Classes in the RACM Gas Chemistry Contributing to SOA Formation, Their OH Rate Constants, and Simulated Averaged Summer Weekday Emissions for the United States East of 104°W Longitude

RACM Species	Description	OH Reactivity at 298°K (cm^3 $molecule^{-1}$ s^{-1})	Emissions (kmole h^{-1})
HC5	Alkanes with medium OH reactivity (e.g., pentanes)	4.77×10^{-12}	3,200
HC8	Alkanes with high OH reactivity (e.g., octanes)	1.08×10^{-11}	2,060
OLT	Terminal alkenes	3.06×10^{-11}	710
OLI	Internal alkenes	7.12×10^{-11}	970
TOL	Toluene	5.96×10^{-12}	1,230
XYL	Xylene and more reactive aromatics	2.40×10^{-11}	960
CSL	Cresol and other hydroxy substituted aromatics	6.00×10^{-11}	50
ISO	Isoprene	1.01×10^{-10}	22,800
SESQ	Sesquiterpene	2.52×10^{-10}	680
API	Alpha-pinene and other cyclic terpenes	5.37×10^{-11}	3,300
LIM	d-limonene and other cyclic diene-terpenes	1.71×10^{-10}	830

Table 4. SOA Mass Yields [*Murphy and Pandis*, 2009] for the VOC Precursors and Volatility Bins Used in WRF-CHEM[a]

	High NO_x Conditions				Low NO_x Conditions			
VOC	1	10	100	1000	1	10	100	1000
HC5	0.0000	0.0375	0.0000	0.0000	0.0000	0.0750	0.0000	0.0000
HC8	0.0000	0.1500	0.0000	0.0000	0.0000	0.3000	0.0000	0.0000
OLT	0.0008	0.0450	0.0375	0.1500	0.0045	0.0090	0.0600	0.2250
OLI	0.0030	0.0255	0.0825	0.2700	0.0225	0.0435	0.1290	0.3750
TOL	0.0030	0.1650	0.3000	0.4350	0.0750	0.2250	0.3750	0.5250
XYL, CSL	0.0015	0.1950	0.3000	0.4350	0.0750	0.3000	0.3750	0.5250
ISO	0.0003	0.0225	0.0150	0.0000	0.0090	0.0300	0.0150	0.0000
SESQ	0.0750	0.1500	0.7500	0.9000	0.0750	0.1500	0.7500	0.9000
API, LIM	0.0120	0.1215	0.2010	0.5070	0.1073	0.0918	0.3587	0.6075

[a]Yields are for four volatility bins with saturation concentrations of 1, 10, 100, and 1000 $\mu g/m^3$ at 300 K and depend on RO_2/NO_x conditions as described in the text.

(POA, SOA, anthropogenic and biogenic) [*Hildebrandt et al.*, 2011]. Our model does not consider any effect of the acidity of inorganic aerosols on the SOA concentrations [*Hallquist et al.*, 2009]. Equation (1) is solved by the Newton iteration method. In order to calculate the SOA yield for each bin we deploy the following formula:

$$VOC^i \xrightarrow{oxidation} \sum_{n=1}^{4} \alpha_n^i P_n^i \tag{2}$$

where the α_n^i yields are

$$\alpha_n^i = B\alpha_n^{i,\,high} + (1-B)\alpha_n^{i,\,low} \tag{3}$$

and VOC^i is VOCs from different classes (Table 4). The VOCs are oxidized by reacting with hydroxyl radical (OH), ozone (O_3) or nitrate radical (NO_3) and the reactions produce organic mass (P_n^i) for all bins (dependent on the yields, equation (3)), which are subsequently partitioned into aerosol and gas phase using equation (1). The mass-based stoichiometric yields are different for two regimes, high and low NO_x conditions (Table 4). The model calculates the final yield by using (3), where B, branching ratio, is defined as in the work by *Lane et al.* [2008b]. This parameter determines the fraction of organoperoxy radicals that react with NO as opposed to HO_2 and other organoperoxy radicals.

[18] The VOCs forming SOA are divided into two groups, anthropogenic and biogenic. Isoprene, monoterpenes and sesquiterpenes (last four rows in Table 3) are emitted by biogenic sources, while other VOCs by anthropogenic sources. Correspondingly, the aerosols formed by oxidation products of these two classes are named anthropogenic (ASOA) and biogenic SOA (BSOA). Although isoprene has a small anthropogenic contribution, the anthropogenic emissions of isoprene are orders of magnitude lower than its biogenic counterpart, thus it is considered biogenic within our classification. 2-Methyl-3-Buten-2-ol (MBO) was separated from the terminal alkenes class (Table 3), since it is biogenic and has high fluxes in the western United States. As laboratory measurements indicate, the SOA yield from MBO is very low compared to anthropogenic terminal alkenes [*Chan et al.*, 2009]. Therefore, MBO is treated as a separate species in the gas phase chemistry and atmospheric transport.

[19] Since the RACM [*Stockwell et al.*, 1997] mechanism within WRF-CHEM does not include sesquiterpenes, this class was added in order to take into account its contribution to SOA production. The chemical reactions for sesquiterpenes are implemented as in the work by *Papiez et al.* [2009] within the RACM mechanism of WRF-CHEM.

[20] The new SOA mechanism contains four volatility bins for each SOA class, and their organic vapors that can condense on aerosol phase. Equilibrium between gas and particle phase matter for each bin is assumed in the model. The SOA species are added within the MADE aerosol module, which considers composition within the Aitken and the accumulation modes separately. The updated WRF-CHEM model therefore requires a minimum of 8 SOA and 8 OCVs, which are fully advected and mixed by boundary layer and cumulus convection parameterizations during the model run. This compares with 16 SOA species and 8 OCVs in the original *Schell et al.* [2001] formalism within standard WRF-CHEM. For diagnostic purposes the ASOA and BSOA species are separated within the simulations, advecting them as separate substances, therefore requiring 16 SOA species for this study.

[21] In our model the dry deposition velocity of the OCVs is parameterized as proportional to the model calculated deposition velocity of a very soluble gas, nitric acid (HNO_3). The parameter which determines the fraction (denoted as "depo_fact") of HNO_3 is assumed in the model since no observation constraints are available. The dry deposition velocity of HNO_3 is calculated by the model during runtime. The dry deposition of gas phase species in WRF-CHEM is parameterized according to *Erisman et al.* [1994], while for particles the Wesely approach [*Wesely and Hicks*, 2000] is used. The version of the WRF-CHEM model used here (version 3.1.1) does not have a wet deposition scheme appropriate to our study. Therefore this work does not consider wet removal processes.

[22] Laboratory studies [*Kroll et al.*, 2007; *Ng et al.*, 2006] indicate that the OCVs from the first generation VOC oxidation products may undergo further oxidation processes by reacting with the hydroxyl radical. Such oxidation generally reduces the vapor pressure of those species, thus shifting mass from high volatility bins to lower ones [*Tsimpidi et al.*, 2010]. For example for anthropogenic OCV species such photochemical aging occurs as follows:

$$VASOA_n + OH \rightarrow 1.075\ VASOA_{n-1} \tag{4}$$

Here $VASOA_n$ denotes anthropogenic OCV for bin n. These reactions are implemented within the model's gas chemistry scheme by using the oxidation rate of 1×10^{-11} cm^3 molec.$^{-1}$ s^{-1} [*Murphy and Pandis*, 2009], and the 7.5%

Table 5. Settings for the Different WRF-CHEM Runs

Sensitivity Runs	Description
R1	no aging, depo_fact = 0.25
R2	aging of biogenic OCVs only, depo_fact = 0.25
R3	aging of anthropogenic OCVs only, depo_fact = 0.25
R4	aging of anthropogenic and biogenic OCVs, depo_fact = 0.25
R5	as R4, but SOA yields are reduced by 50%
R6	as R4, but depo_fact = 0.5
R7	as R4, but depo_fact = 0.75
R8	as R4, but depo_fact = 1.0
R9	as R4, but aging rate for OCVs is reduced by 50%
R10	as R4, but MYJ PBL scheme
HR1	as R1, but the 20 km resolution domain
HR4	as R4, but the 20 km resolution domain
HR6	as R6, but the 20 km resolution domain

increase is due to addition of oxygen atoms. We apply similar aging reactions for biogenic OCVs. To be consistent with other authors doing VBS modeling, we also use here the "aging" term for homogeneous oxidation of OCV by OH radical, although in the traditional literature this term is usually applied to the heterogeneous reactions of aerosol particles.

[23] There are several key differences between our modeling settings and previous modeling studies based on the VBS approach. First, most of the aforementioned SOA model developments were focused on Mexico City [*Hodzic et al.*, 2010; *Shrivastava et al.*, 2011; *Tsimpidi et al.*, 2010] or global scale using course model resolution [*Farina et al.*, 2010; *Pye and Seinfeld*, 2010]. Second, the studies for the eastern United States using the PMCAMx model [*Murphy and Pandis*, 2009, 2010] included emissions of intermediate volatility organic compounds as additional SOA precursors that are believed to be missing from current emission inventories. In our model we consider only traditional SOA precursors; VOCs listed in Table 3. Third, we use the WRF-CHEM model, which performs simultaneous meteorological and chemical simulations during the integration time. Advantages of using WRF-CHEM compared to offline models such as PMCAMx [*Murphy and Pandis*, 2009] include the tight coupling between meteorology and constituent transport, also the consistency between physical parameterizations used in radiation, PBL dynamics, mixing, convection and photolysis simulations. Fourth, our modeling domain covers the entire continental United States (Figure 1), which considers the influence of the western part of the continent to the eastern region. Also, we do not impose any lateral boundary conditions for OA, since the east and west boundaries are over open-ocean and transboundary flows of OA are highly uncertain. In our model setup all OA is either emitted within the simulated domain as nonvolatile POA or formed by secondary oxidation processes.

[24] The vertically stretched WRF-CHEM grid extends to the tropopause. Though the upper troposphere does not play a significant role in OA formation, it allows accounting for convective mixing of the tracers to upper layers. The vertical resolution is $\sim$10 m near the surface, where about 20 layers are located within the lowest 2 km. The PM2.5 composition measurements made at the surface stations usually are taken few meters above ground. Concentrations of chemical species are assigned at the center of each vertical layer by the model. Consequently contrasting the simulated concentrations with the near surface measurements make a high vertical resolution necessary. This is especially crucial for the comparison using the nighttime data, since nocturnal PBL is usually very shallow. Moreover the finer vertical resolution in higher altitudes is important to capture the PBL structure and for better comparison with the aircraft data from TexAQS-2006.

2.2. Different Model Scenarios

[25] We simulated meteorological and chemical species for the continental United States using the WRF-CHEM model with different configurations (see Table 5). The first 10 model runs are for 60 km resolution, and the remaining three are for the 20 km resolution domain. All of the runs have the same base model configurations as listed in Table 2, except a few differences outlined in Table 5. The simulation scenarios may be grouped as follows: (1) base case without aging of the OCVs, named as "R1"; (2) aging of the OCVs, R2, R3 and R4 runs; (3) enhanced dry deposition for the OCVs, R6, R7 and R8 runs; (4) reduced SOA yields, R5; (5) slower aging rate, R9; (6) parameterization of vertical mixing, R10; and (7) 20 km resolution domain, HR1, HR4 and HR6.

[26] The model runs are constructed so the influence of some key uncertainties in the SOA mechanism can be examined. We do the R10 run with a different Planetary Boundary Layer (PBL) scheme Mellor-Yamada-Janjic [*Mellor and Yamada*, 1982] to examine the difference in SOA fields due to the uncertainties in the vertical mixing parameterization.

[27] Three model runs (denoted as HR*) use the same settings as their 60 km counterpart (e.g., HR1 and R1), but are done at 20 km resolution for the same time period. The purpose of these high-resolution runs is to study the sensitivity of the different SOA mechanisms to the model resolution. Though 60 and 20 km resolution domains are somewhat different in size, the comparisons and analysis of the results are made for the same area and observations. The capability of doing 20 km resolution simulations is limited due to higher computational cost (machine time and memory storage).

[28] For evaluation we select the time period from 4 August to 28 September (56 days) 2006, where the model outputs for 1 through 3 August are used for spin-up. The model runs are performed for each day by initialization of the meteorology at 00 UTC by using the GFS analysis, while all the chemical species are passed from the previous day's WRF-CHEM run output. Idealized vertical profiles for some chemical species are used for initialization at the beginning of the simulation period, and continuously for their lateral boundary conditions.

[29] In Figure 1 we show the surface OA distribution for the 20 km resolution WRF grid, averaged over the study period. The results are based on the HR6 run, which, as shown below, agrees reasonably well with most of the observations. We see high OA concentrations ($\approx$7 μg/m^3) in the southeast United States mostly due to high SOA formation in this area. Increase in OA concentrations over water in the vicinity of the east and in the southeast coastal regions is attributed to the aging mechanism and also shallow mixing over water. Enhanced OA concentrations associated with populated northeast and west coast cities are apparent as well. OA levels are less over the Great Plains, and northern

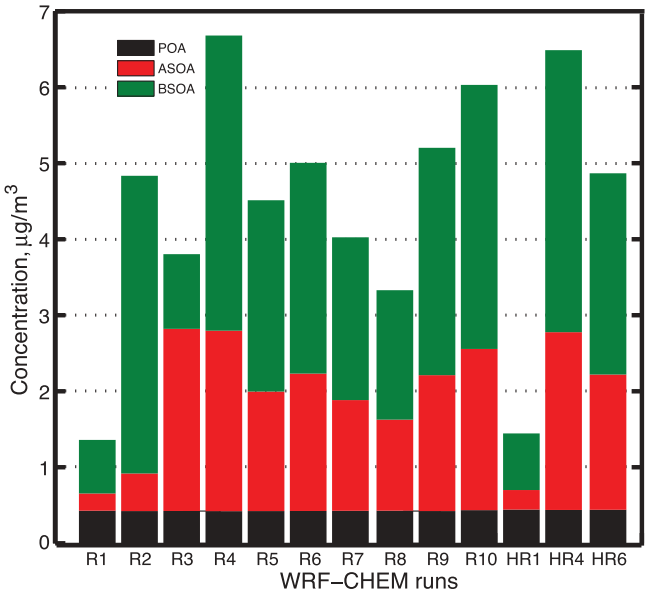

Figure 2. OA composition from all the model scenarios. The numbers are concentrations of the species at 20 UTC but averaged for all days during the evaluation time period and within the space encompassed by the nested grid in Figure 1.

U.S. states. It should be emphasized that predicted summertime OA distribution in the forested western United States does not include the effects of wildfires that were active during the summer of 2006.

[30] A nested grid shown in blue is embedded in Figure 1, which encompasses a region with high OA concentrations in the eastern United States. To analyze the WRF-CHEM predicted OA components within that nested grid, we present the averaged near surface concentrations of POA, ASOA and BSOA species from all the model runs in Figure 2. The diagrams in Figure 2 demonstrate the magnitude of the modeled OA and contribution of different OA sources (primary, secondary anthropogenic and biogenic) to the total concentrations during local afternoon, when SOA production is high. The plot reveals major differences in the SOA species from different simulations. The spatially and temporally averaged POA concentrations, which are on average ≈0.4 $\mu g/m^3$ are almost same among all runs, even those with different resolution and PBL scheme. Unlike POA, mean ASOA and BSOA concentrations vary significantly between the runs depending on aging and other settings. The differences in SOA between the 60 and 20 km runs with the same settings are small, indicating over this range the grid size do not matter. Although the strong emission sources are better resolved in 20 km domain, this does not lead to significant enhancements in large-scale POA and SOA distributions within the region of interest. Interestingly, the SOA concentrations are smaller in the R10 run compared to R4, though the runs use the same settings but different PBL schemes. There is a slight increase in BSOA when anthropogenic OCVs only are aged (R3 versus R1) due to the nonlinear partitioning within equation (1). Also we find that in the base cases (R1 or HR1) the role of BSOA in SOA is dominant. This feature is opposite if anthropogenic OCVs only are aged (the R3 run). Otherwise the total fraction of BSOA within the eastern United States is somewhat higher than ASOA if we assume the multigenerational oxidation for biogenic VOCs (Figure 2).

2.3. Surface Observations

[31] We evaluate the model runs using available long-term aerosol speciation measurements in the United States. Though our model domain encompasses the western United States (west of longitude 104°W), in our evaluations we neglect that region for two reasons. First, there were significant forest fires in the Northwest United States in the summer of 2006, which is obvious in the network observations (figure not shown), and are frequent in the northwest United States during summer [*Spracklen et al.*, 2007]. Second, the SOA dominant region in the United States is believed to be the eastern part of the country, especially the southeastern region [*Goldstein et al.*, 2009], where air quality models traditionally have difficulties in simulating observed values of OA and $PM_{2.5}$.

[32] Data from three surface aerosol speciation networks were used for model evaluation. All three networks measure OC and EC in the $PM_{2.5}$ size range using continuous analyzers or filter-based samplers. These are the EPA's Speciation Trends Network (STN) (http://www.epa.gov), the Interagency Monitoring of Protected Visual Environments (IMPROVE) (http://vista.cira.colostate.edu/improve) and the Southeastern Aerosol Research and Characterization (SEARCH) (http://www.atmospheric-research.com/studies/SEARCH/index. html) networks.

[33] The IMPROVE monitoring program is used primarily to track long-term temporal changes in visibility at national parks, consistent with the needs of the Regional Haze Rule [*Malm et al.*, 2011]. The $PM_{2.5}$ speciation target analytes for IMPROVE and STN monitoring networks are similar and consist of an array of 74 ions, carbon species, and trace elements. Each series of analytes requires sample collection on an appropriate filter medium to allow chemical analysis with methods of adequate sensitivity. The methods used for analysis of these filter media include controlled combustion thermal optical transmittance and reflectance for carbon analysis of particulate matter. Most of the IMPROVE surface sites are located in rural areas, while the STN sites are mainly located in urban areas. Both networks cover the entire country. The STN and IMPROVE networks provide 24 h averages of various components of the aerosol mass. The filter samples usually are taken every third day.

[34] The third network, SEARCH, consists of eight research sites located in the southeastern United States. The SEARCH network has been in operation since 1998 and was designed to collect long-term data on trace gases (e.g., O_3, SO_2, NO_y), particle mass and composition ($PM_{2.5}$ and PM_{10}) and surface meteorology at paired urban-rural sites in and around the cities of Atlanta, GA; Birmingham, AL; Pensacola, FL and Gulfport, MS [*Hansen et al.*, 2003]. The great advantage of the SEARCH network is the availability of hourly measurements, allowing evaluation of the diurnal cycles for simulated OC and EC [*Hansen et al.*, 2006]. A detailed description of all three networks, deployed measurement standards and techniques can be found in the work by *Chow et al.* [2010].

[35] The IMPROVE data provided to the research community is blank corrected to take into account positive

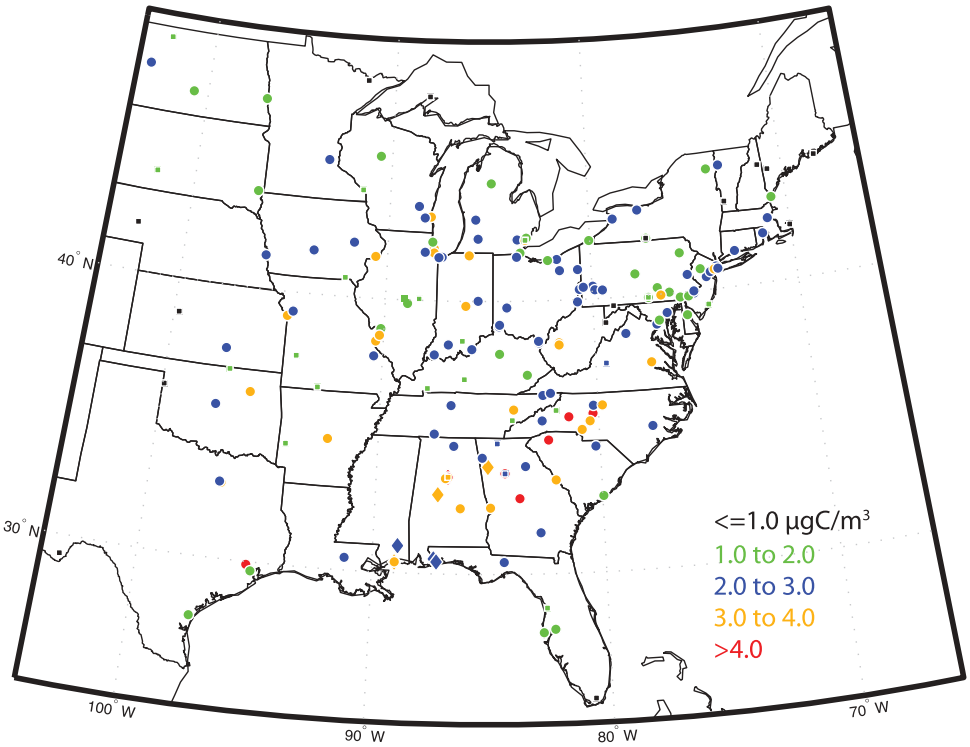

Figure 3. Observed daily OC concentrations (medians) at the IMPROVE, STN, and SEARCH sites from 4 August to 28 September 2006. There are 37 IMPROVE, 134 STN, and 7 SEARCH sites with valid OC data. The IMPROVE, STN, and SEARCH sites are depicted using square, circle, and diamond shapes, respectively.

artifacts related to sample handling and analysis. Nevertheless a recent study by *Malm et al.* [2011] suggests that due to the flow rate of the samplers the IMPROVE technique may underestimate ambient OC concentrations by ≈20%. Comparisons between the IMPROVE and STN reported OC data have revealed that the STN OC data needs to be blank corrected in order to be consistent with the IMPROVE OC data [*Chow et al.*, 2010]. Therefore, we applied blank corrections for all the STN sites following the approach of *Chow et al.* [2010]. These artifacts are ≈1 μgC/m^3 for each station for the modeling time period.

[36] For the IMPROVE and STN networks we applied the following data selection criteria: a minimum of 8 days of valid measurements must be available within the time period of 4 August to 28 September for the IMPROVE and STN data. The SEARCH sites provide measurements almost every day and hour, and we have chosen data selection criteria requiring at least 20 h a day to calculate a diurnal average for a given site and minimum 35 of valid daily points for a given site. Due to insufficient OC data the SEARCH site in downtown Atlanta, GA is not included in this study.

[37] Figure 3 shows medians of daily averages of OC (after filtering is applied) in the eastern United States observed at all three networks. The spatial coverage, the range of observed OC concentrations, and the spatial variability of the reported OC from all the networks can be inferred from the plot. We also present medians of the daily averages for OC and EC for three networks separately in Table 6, since these species are used in the model evaluation below. In addition we provide the total number of the sites and days (Table 6) for each network, for which the valid measurements are available. The STN network reports higher OC values (after blank corrections) than IMPROVE sites despite the fact that both networks cover a similar size of the domain. One reason for this is that IMPROVE sites are predominantly in rural locations versus STN sites in urban areas; different measurement approaches may also

Table 6. Median Concentrations of OC and EC for the Three Surface Networks During the Period From 4 August to 28 September 2006 for Network Sites East of 104°W Longitude Meeting the Data Criteria Described in the Text[a]

			Number of Sites Meeting Criteria		Number of Valid Points	
Network	OC (μgC/m3)	EC (μg/m3)	OC	EC	OC	EC
IMPROVE	1.09	0.29	37	37	621	619
STN	2.48	0.53	134	132	1508	1493
SEARCH	3.39	0.34	7	7	338	340

[a]Daily values for the SEARCH sites are 24 h averages of the hourly concentrations.

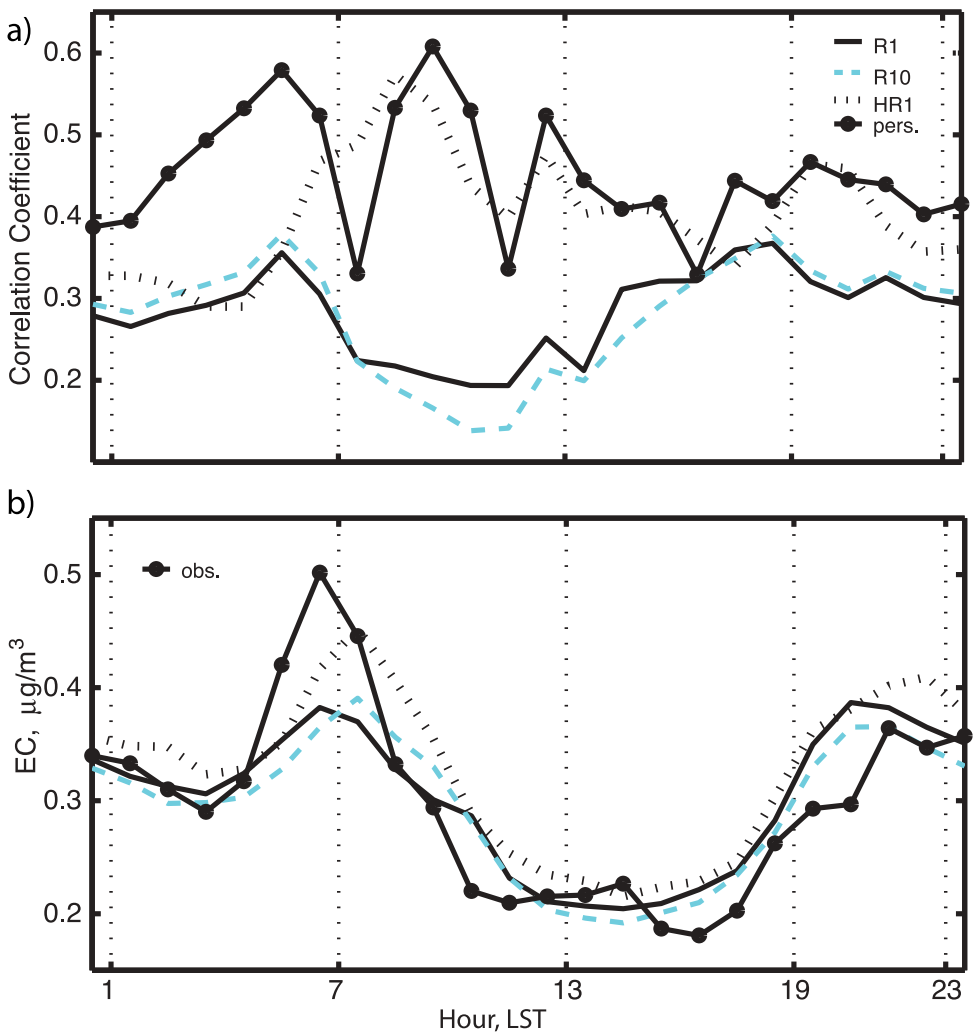

Figure 4. Model-observation comparison of the hourly EC concentrations at the SEARCH sites. (a) Correlations, "pers" stands for persistence forecast. The correlations are calculated by lumping together the concentrations from all sites and days for every hour. (b) The diurnal cycles are medians of the EC values for all stations from 4 August to 28 September 2006.

play a role, as noted earlier. The SEARCH network covers both rural and urban areas in the southeast United States, a region relatively "rich" with OC, showing high (median OC ≈3.4 μgC/m^3) concentrations. Here three of the SEARCH sites are located in urban areas and others are in rural and suburban areas. The highest daily OC concentrations (median OC ≈5 μgC/m^3) are reported at the SEARCH site located 3 km north of Birmingham, AL (Figure 3). A rural site, Yorkville, located west northwest of Atlanta, GA, also is also prominent in terms of high OC (median OC ≈3.8 μgC/m^3) despite its classification as rural.

3. Discussion of the Results

3.1. Evaluation of the Model Using the Surface Data: Hourly Concentrations

[38] We evaluate the model performance by comparing EC and OC individually for each network. As mentioned earlier the networks cover different regions and target different sources, therefore the evaluation for all three networks is reported separately. It is important to first quantify the model's skill in resolving the diurnal cycle of the species, since this has implications for using daily averages in the model evaluation. Unfortunately, only the SEARCH network provides the possibility of evaluating the simulated hourly OC and EC values.

[39] In order to evaluate the model OA species we hereafter use total mass to total carbon mass ratios (so-called OM:OC ratios) of 1.4 and 2.0 (μg/μgC) to convert model POA, and SOA components, respectively [*Murphy and Pandis*, 2009]. These OM:OC ratios are also consistent with the recent study of *Simon et al.* [2011], who estimate a summertime mean OM:OC ratio of 1.85 for the eastern United States using data from the IMPROVE network. Nevertheless there are uncertainties in using a constant ratio, since this ratio for SOA depends on its oxidation level and type.

[40] We first compare EC simulations from the model and the observations, since EC is a passive tracer, it is generally coemitted with POA, and it coexists with OC within fine particles (Figures 4a and 4b). We show only three runs,

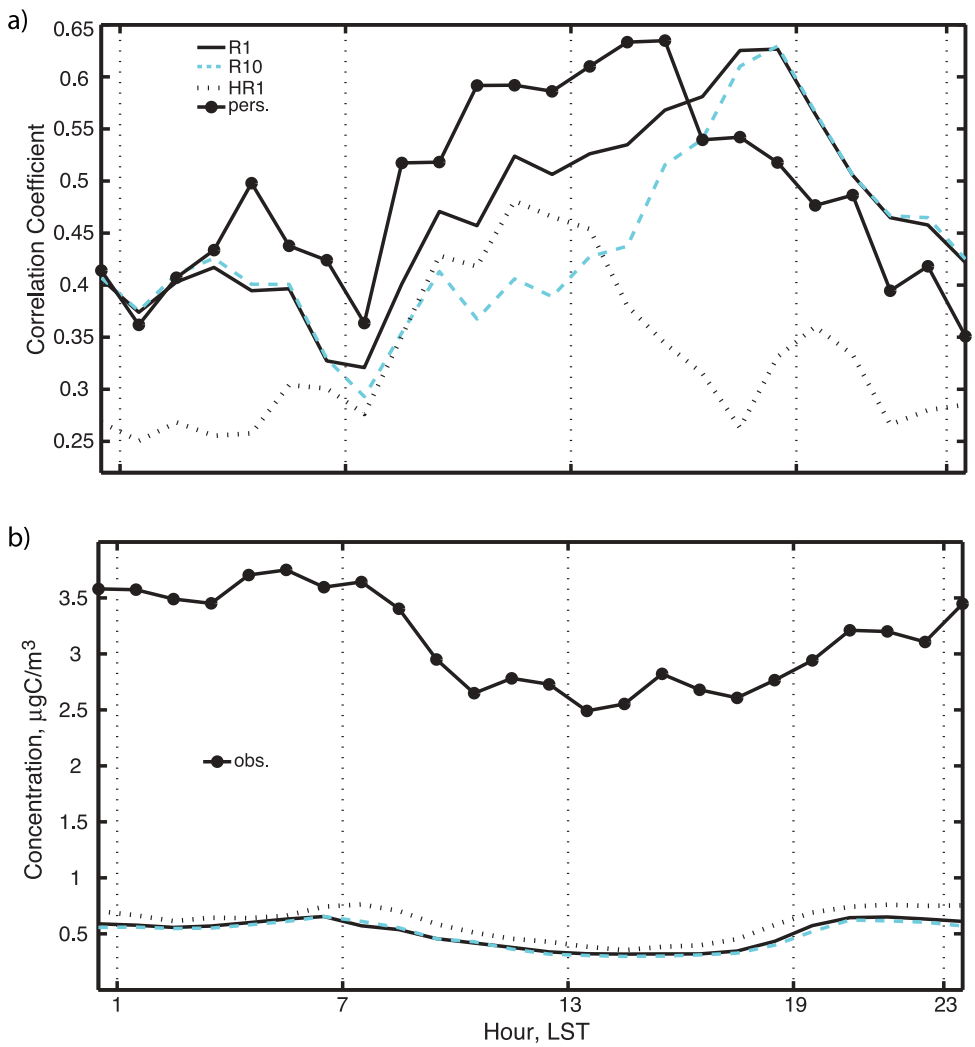

Figure 5. Model-observation comparison of the hourly model POA and OC concentrations at the SEARCH sites. (a) Correlation, "pers" stands for persistence forecast. (b) Concentrations, which are medians of the values for all stations from 4 August to 28 September 2006.

since the EC fields are the same for other runs, R2–9 are the same as R1, while HR4 and HR6 the same as HR1. Simulated EC concentrations can vary due to the PBL scheme and the model resolution. As an objective benchmark for forecast performance, correlations for the persistence forecast of EC are also shown in Figure 4a, which is calculated by comparing the previous day's hourly EC values for a given day at the same hour. The purpose of including persistence is to verify the model's skill in prediction. As Figure 4a shows the overall correlations of the persistence or the model are small for hourly EC. The 20 km resolution domain captures day-to-day variability of EC much better than the 60 km runs. Figure 4b shows the median diurnal cycle for EC at the SEARCH sites and three model runs. All the model runs simulate the diurnal variability in EC reasonably well except for a 4 h period in the early morning. The 20 km resolution simulation (HR1 case) overestimates EC values slightly compared to the 60 km runs, but does a better job of simulating the strong early morning increase in EC. These results underline the advantage of the higher resolution, which should enable better resolved transport, mixing and the emission sources. Since EC is only influenced by emissions, transport and deposition, the agreement between model and observations shown in Figures 4a and 4b suggests the model is representing the interaction of these three processes reasonably well, and diurnal averages are not significantly compromised by possible model deficiencies within these three processes.

[41] Figures 5a and 5b show similar hourly correlation and diurnal cycle for model POA versus observed OC. This is an important comparison, since the standard WRF-CHEM with MADE/SORGAM aerosol module predicts OA almost entirely as POA due to very little SOA formation from the *Schell et al.* [2001] formulation. It is clear that the default model without proper inclusion of SOA formation severely underestimates the OC concentrations in the southeastern United States throughout the day regardless the model resolution or the PBL scheme. Also, the correlations are quite low compared to persistence for most hours of the day.

[42] Figures 6a and 6b show the analogous hourly correlation and diurnal cycle for model OC versus observed OC, and for all model cases listed in Table 5. Figure 6a shows

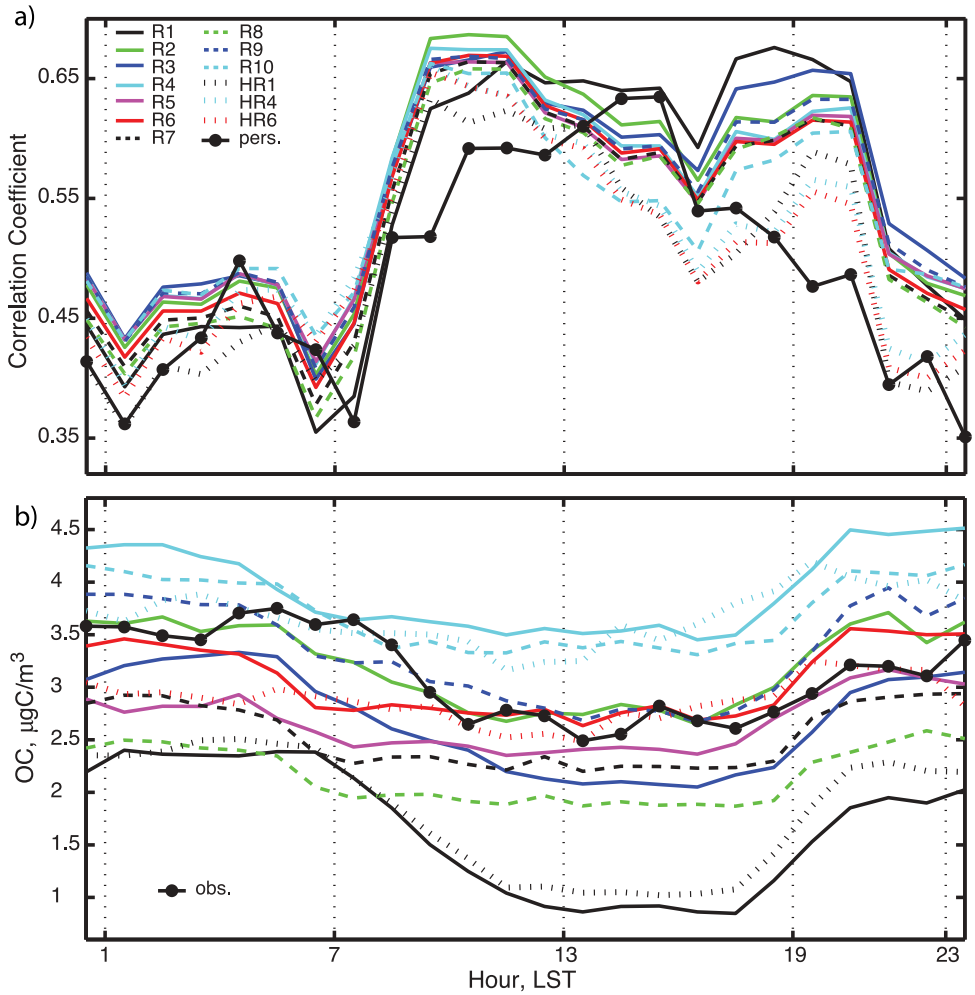

Figure 6. Model-observation comparison of the hourly OC concentrations at the SEARCH sites. (a) Correlations, "pers." stands for persistence forecast. (b) Concentrations, which are medians of the values for all stations from 4 August to 28 September 2006.

relatively low correlations in the night with sharp increases after sunrise for persistence and the model runs. All model cases exhibit good correlations (≈0.6–0.7) and exceed the persistence correlation between 9:00 and 13:00 local standard time (LST), with larger correlation discrepancies between the runs apparent between 13:00 and 23:00 LST. A possible factor affecting diurnal correlations may be the location of the SEARCH sites. Three of them are located in close proximity to the Gulf of Mexico and their accurate representation may require much finer model horizontal resolution ~2 km to resolve the land-water contrast interface. Though the overall correlations for hourly OC are not high, the majority of the model runs beat persistence in correlation, especially in the morning and evening hours. Comparison with the POA only case in Figure 5a highlights the increased skill of the model in capturing the variability in atmospheric OC when the SOA formation mechanism is included. Note also that afternoon to evening correlation statistics are degraded with the use of the MYJ PBL scheme. The 20 km resolution OC correlations are also degraded relative to the 60 km resolution runs during this time period, contrary to EC correlation coefficients significantly increasing with the finer resolution (Figure 4a). This suggests that finer-scale (~20 km) SOA phenomena may be missing in the formalism. As discussed further below, biogenic sources dominate the OA predictions at the SEARCH sites, which suggests refinements in the treatment and sources of biogenic SOA may still be needed.

[43] Figure 6b shows much larger variability among the model median concentrations compared to the correlations in Figure 6a. While a few runs are able to simulate the observed medians of OC reasonably well, some model scenarios considerably underestimate the magnitude of OC throughout the day. The R1 and HR1 runs can explain only ≈ 30% of the observed OC concentrations during midday, showing the impact of neglecting the OCV aging process. Comparison of Figure 6b with Figure 5b reveals how much model SOA contributes to total OC for different runs. The R2, R4, R9–10 and HR4 runs simulate the OC concentrations with little bias for most of the day. HR6 and HR4 show similar diurnal cycles, but the increased deposition rate in HR6 yields better agreement with the observations, especially during the daytime.

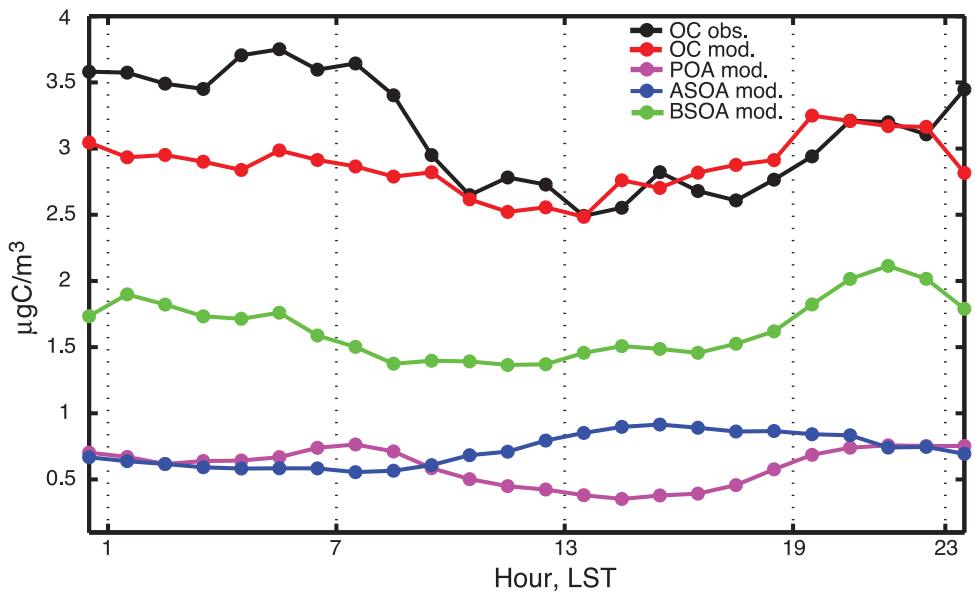

Figure 7. Median of the diurnal cycle of the observed OC at the SEARCH sites and the simulated (the HR6 run) OA, POA, ASOA, and BSOA (all are in carbon mass) from 4 August to 28 September 2006.

[44] We picked one model case, HR6, to illustrate how different OA components contribute to the modeled hourly OC at the SEARCH sites. Figure 7 shows median of the diurnal cycle for the hourly SEARCH data together with simulated OA, POA, ASOA and BSOA. The diurnal cycle of OC shows concentrations reaching a maximum in the night and early morning. In the model this is mainly caused by nighttime SOA production and accumulation of the particles in the shallow nocturnal boundary layer. At the urban sites nighttime accumulation of POA emitted by nearby sources (mainly traffic) contributes to nocturnal OA buildup too. The POA concentrations are small, and they vary from highest values during early morning to the lowest in the afternoon. The total OC from the model agrees well during daytime, however it underestimates OC in the night and early morning hours by ≈ 15–20%. Model ASOA concentrations are close to POA in the night, but increase during the daytime. BSOA is the dominant contributor to the modeled OC throughout the day, and BSOA enhances during night due to BSOA formation from terpene reactions with O_3 and NO_3 and their accumulation in the shallow PBL. This buildup of nighttime BSOA from terpenes is a large-scale model feature associated with coniferous forests throughout the model domain.

3.2. Evaluation of the Model Using the Surface Data: Daily Concentrations

[45] The $PM_{2.5}$ National Ambient Air Quality Standards established by the EPA are based on 24 h and annual average concentrations. It is therefore important to compare model and observed diurnally averaged OA, since organic matter comprises a significant fraction of $PM_{2.5}$. The spatial coverage of the IMPROVE and STN networks provides an opportunity to assess model capability in SOA simulations over a large region. In this section the model scenarios are evaluated using the daily EC and OC from the IMPROVE and STN networks for the eastern United States with the SEARCH statistics included for completeness.

[46] Table 7 provides detailed quantitative statistics for daily EC comparisons for all of the model scenarios. The r values vary from low for the IMPROVE network to a little higher for the SEARCH sites. The model underestimates EC concentrations somewhat except for the SEARCH network. For the STN sites higher resolution seems to help improve the EC model bias slightly. The impact of the MYJ PBL scheme (R10 run) is small for IMPROVE and STN sites, while for the SEARCH network it results in lower correlation and more underestimation. Comparisons for EC show a small but statistically significant improvement due to the increased horizontal resolution in the 20 km case, and likewise for the hourly EC comparisons at the SEARCH sites.

[47] Tables 8a, 8b, and 8c provide statistics of the OC comparisons for all the 13 model cases versus all 3 networks similar to EC. From Table 8a it indicates that most model runs overestimate on average the OA concentrations at the IMPROVE sites, though the runs without aging (R1, HR1) show large negative bias at all sites, emphasizing that without aging of OCVs we cannot simulate the OC concentrations properly. In general the STN and SEARCH sites show

Table 7. Statistics of 24 h-Averaged EC Comparison for the Three Networks for Monitors East of 104°W Longitude Meeting the Data Criteria Described in the Text[a]

Networks	Model Runs	r	MB ($\mu g/m^3$)	MMO
IMPROVE	R1	0.47	−0.09	0.71
	R10	0.46	−0.09	0.65
	HR1	0.50	−0.10	0.65
STN	R1	0.54	−0.16	0.77
	R10	0.49	−0.14	0.79
	HR1	0.62	−0.09	0.85
SEARCH	R1	0.58	−0.04	0.87
	R10	0.57	−0.05	0.82
	HR1	0.65	−0.03	0.89

[a]Here r, correlation coefficient; MB, mean bias; MMO, median of model over observation. Medians of MMO and MB are given.

Table 8a. Statistics of 24 h-Averaged OC Comparison for the IMPROVE Network for Monitors East of 104°W Longitude Meeting the Data Criteria Described in the Text

Model Runs	r	MB (μgC/m^3)	MMO
R1	0.55	−0.45	0.64
R2	0.64	0.64	1.53
R3	0.59	0.29	1.27
R4	0.62	1.30	2.03
R5	0.60	0.48	1.40
R6	0.61	0.56	1.46
R7	0.61	0.20	1.16
R8	0.59	−0.09	0.89
R9	0.62	0.77	1.66
R10	0.65	1.01	1.91
HR1	0.58	−0.44	0.67
HR4	0.63	1.25	1.90
HR6	0.61	0.52	1.39

Table 8c. Statistics of 24 h-Averaged OC Comparison for the SEARCH Network for Monitors Meeting the Data Criteria Described in the Text

Model Runs	r	MB, μgC/m^3	MMO
R1	0.73	−1.77	0.53
R2	0.75	−0.20	0.91
R3	0.76	−0.88	0.77
R4	0.76	0.57	1.08
R5	0.76	−0.91	0.75
R6	0.74	−0.46	0.83
R7	0.73	−1.04	0.69
R8	0.71	−1.47	0.59
R9	0.76	−0.12	0.93
R10	0.75	0.19	1.03
HR1	0.68	−1.76	0.52
HR4	0.73	0.48	1.05
HR6	0.72	−0.55	0.79

stronger temporal and spatial variability of OC than the IMPROVE sites, likely due to their proximity to the urban areas (Figure 3). For some model runs (e.g., R5, R6, HR4 and HR6) the median model to observed ratios (MMOs) show that the model predicts the observed values within ±25% for median conditions for the STN and SEARCH sites. Since the spatial coverage of the SEARCH sites is much smaller than other two surface networks, generally this network shows different characteristics than other two. The predominant feature in Table 8a is the overprediction of OC for the IMPROVE network relative to other two surface networks. As noted earlier the IMPROVE network may underestimate the OC concentrations by ≈ 20%, which could lead to the model overestimation for OC. As Table 7 shows the EC comparison for IMPROVE network does not exhibit such model-observation bias, suggesting that the transport of the particles is reasonably well simulated by the model.

[48] All the sensitivity runs exhibit similar correlations with the ambient data with values, ranging from 0.54 to 0.75 for the different networks. The runs with aging of OCVs slightly improve the correlations. This improvement is almost the same for the IMPROVE and STN networks, while not as much for the SEARCH sites. The correlations increase when the VBS mechanism includes aging of biogenic OCVs (R2 versus R1), with almost half of the variance explained by the model in this case. When anthropogenic OCVs only are aged (R3), the correlation slightly drops for IMPROVE and STN, while there is a little improvement for SEARCH. Since OA concentrations are largely influenced by chemical processes involved in SOA formation, the increased resolution may not always result in better correlations (HR* runs versus R*) and this could also be due to the representation of spatial variability of the biogenic VOC fluxes.

Table 8b. Statistics of 24 h-Averaged OC Comparison for the STN Network for Monitors East of 104°W Longitude Meeting the Data Criteria Described in the Text

Model Runs	r	MB (μgC/m^3)	MMO
R1	0.61	−1.44	0.42
R2	0.72	−0.31	0.86
R3	0.65	−0.62	0.73
R4	0.68	0.27	1.10
R5	0.67	−0.45	0.80
R6	0.68	−0.40	0.81
R7	0.67	−0.74	0.67
R8	0.65	−1.01	0.58
R9	0.67	−0.18	0.91
R10	0.67	0.15	1.03
HR1	0.63	−1.28	0.49
HR4	0.65	0.33	1.11
HR6	0.66	−0.29	0.86

[49] The MB and MMO values from the Tables 8a, 8b, and 8c illustrate how the simulated SOA fields are sensitive to the various settings of the SOA mechanism and removal of OCVs, since the largest variability between the model results appear in the biases rather than correlations. The runs R4, R6, R7 and R8 are the same model scenarios but with increased deposition rates for OCVs. Though the depo_fact is increased by a factor of 4 from the R4 case to R8, the model observation bias changes only by ≈50%. This suggests a nonlinear dependence of the modeled SOA concentrations on the deposition rate of the OCVs (see also Figure 2). When the SOA yields are reduced by 50% (R5 versus R4), we see ≈30% change in the model bias for all the networks. The reduced aging rate by 50% decreases the SOA concentrations by ≈20% for the daily averages (R4 versus R9).

[50] In order to demonstrate the model-observation comparison in space for the STN network we present Figures 8a and 8b for the HR4 run, which captures the observed OA quite well for this network. The mapped correlation scores show that at some eastern U.S. sites the day to day variability (primarily driven by synoptic variability) of OC is explained quite well by the model (Figure 8a), covering mainly urban Washington-Boston corridor and North Carolina regions. However, the correlations drop for the sites located in the central part of the domain. The 20 km resolution may not be sufficient to capture the temporal variability of OC at several coastal sites located around the Great Lakes and Gulf of Mexico. *Stroud et al.* [2011] found that while the domain-wide average OA concentrations are slightly different between 15 and 2.5 km resolution domains, the high OA levels in urban plumes in the Great Lakes region are better captured in the high-resolution model. Median model OC biases are within ±20% at most of the sites (Figure 8b), even though the spatial variability in the

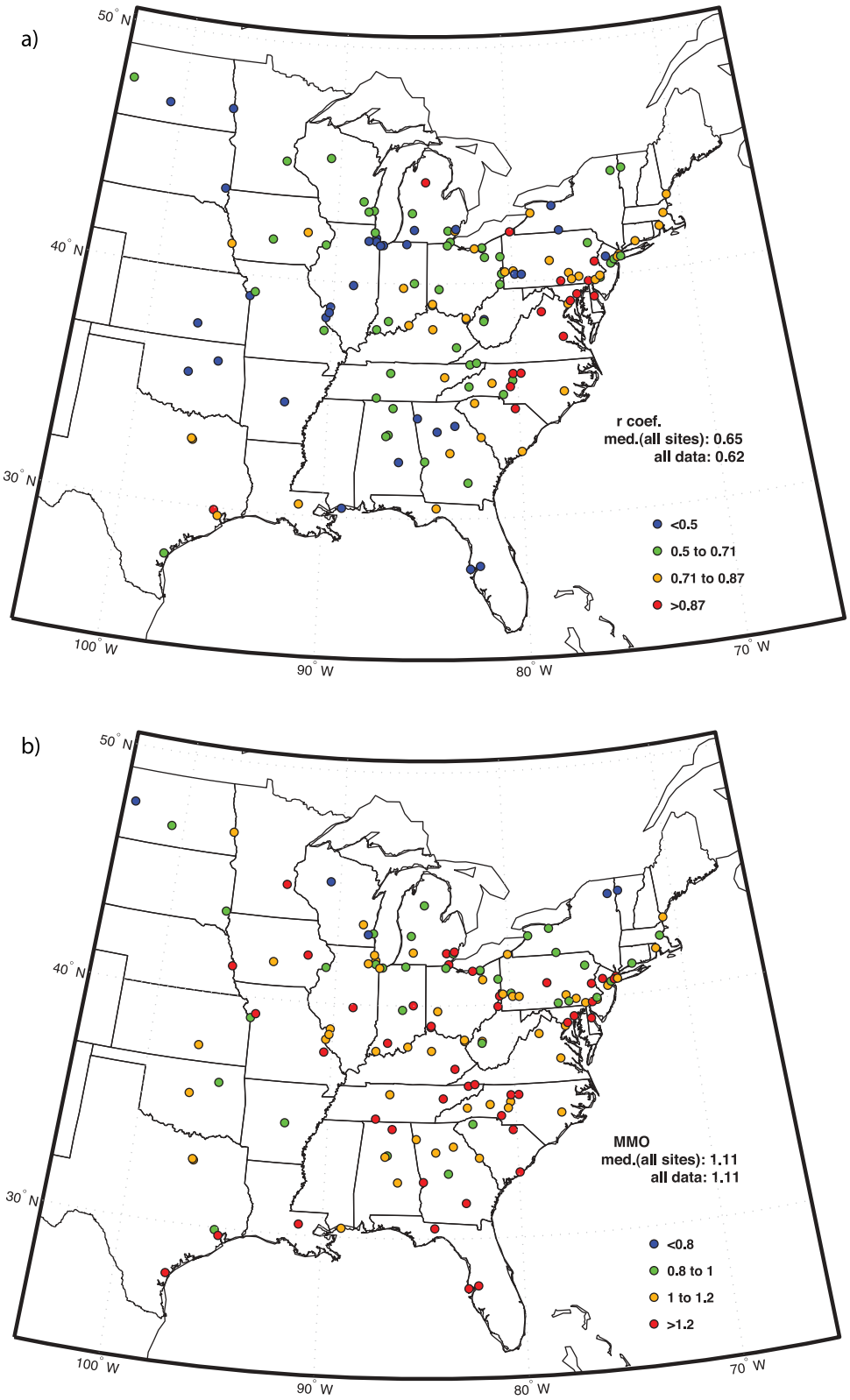

Figure 8. Comparison of the simulated OC from the 20 km resolution WRF-CHEM run (HR4) with the daily averaged OC measurements from the STN network. (a) Correlations and (b) MMOs. Medians of the statistical scores calculated for each site separately ("med. (all sites)") and when all data ("all data") are lumped together are also reported. The first number presents how the model is able to capture the temporal variability of OC. The second number characterizes the model's ability of representing the spatiotemporal variability of OC.

Table 9. Statistics of 24 h-Averaged POA (in Carbon Mass) Comparison With Observed Daily OC at the Surface Networks[a]

	IMPROVE Network		STN Network		SEARCH Network	
Model Runs	r	MMO	r	MMO	r	MMO
R1	0.39	0.25	0.34	0.21	0.73	0.11
R10	0.34	0.25	0.27	0.21	0.70	0.12
HR1	0.45	0.24	0.43	0.25	0.59	0.15

[a]Only runs that are different for POA are shown.

observed OC is much higher (Figure 3). Highest model values show up in a broad region of the southeast United States and in isolated urban areas like Houston, Chicago and New York.

[51] In order to emphasize the impact of SOA on the OA predictions in the eastern United States we present similar statistics of model-observation comparison for POA versus the measured OC in Table 9, with the mean bias values excluded for brevity. Again the statistics for the modeled POA in Table 9 are given only for the R1, R10 and HR1 runs. It is clear that POA alone can only explain <25% (in carbon mass) of the observed surface OC values within the domain. Using a different PBL scheme (R10) or higher resolution (HR1) does not significantly change this conclusion. Additionally, the low correlation coefficients for predicted POA compared to measured OC (see Tables 8a, 8b, and 8c) imply that most of the temporal variability of the OC concentrations is explained by secondary particle mass formation.

[52] Concerning the correlations, it should be noted the model does not include day-to-day variability in anthropogenic VOC and POA emissions, which may also depend on weather and economic activity. Though the weekend versus workday difference in the anthropogenic emissions is taken into account, we did not find any noticeable effect of this on SOA simulations. The study by *Murphy et al.* [2008] has found a marginal weekend/weekday contrast for daily OC concentrations measured by the IMPROVE network.

[53] Figures 9a and 9b show the spatial distributions of the averaged SOA/OA and BSOA/OA fractions, respectively, over the simulation time period for the HR6 run near the surface. For the same model case the averaged OA concentration field is shown in Figure 1. According to Figure 9a the SOA fraction of total OA mass is ≈80–90% for the eastern United States with highest SOA contributions over the southeastern region. There are a number of "spots" where SOA fractions are lower, corresponding to urban and industrial areas with high POA emissions (e.g., Chicago). Aerosol mass spectrometer (AMS) measurements have been used to estimate HOA versus OOA in total OA mass. If we assume HOA in our model would be represented as POA, and SOA as OOA then our modeling results are consistent with different reports [see, e.g., *Zhang et al.*, 2005], where in urban areas POA emissions are strong, and HOA and OOA fractions are ≈30% and ≈70%, respectively.

[54] Figure 9b highlights the contribution of biogenic VOCs to the total OA mass. As noted earlier this contribution is high (≈60%) in the southeastern United States, and the fraction of BSOA decreases to less than 50% toward the northeast part of the country. Also, the BSOA fraction decreases over some big cities. As different field campaigns [e.g., *Bahreini et al.*, 2009; *de Gouw et al.*, 2008] show, there is a strong enhancement of OC over urban areas and downwind. But over large spatial scales biogenic SOA formation likely is the dominant fraction of OA, which is implied from our simulations. Radiocarbon analysis of fine particles taken at some surface locations within the United States found a significant fraction of modern carbon,

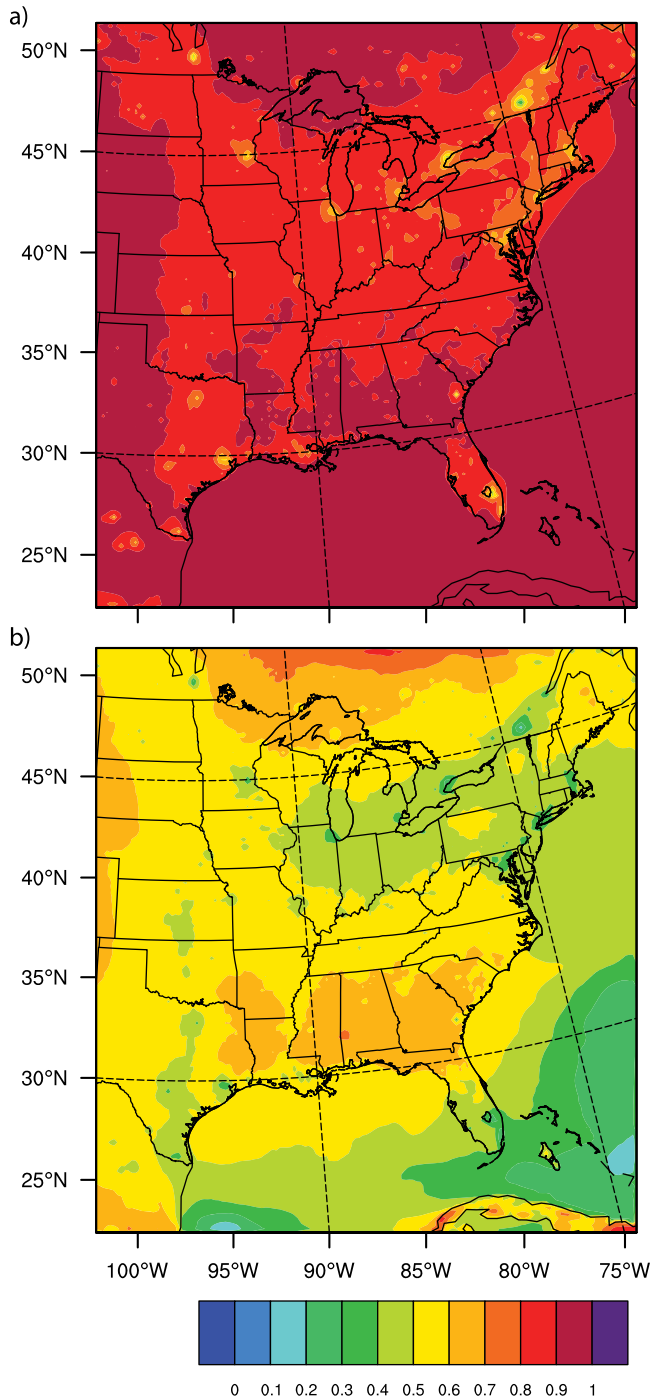

Figure 9. (a) Average SOA over average OA concentration ratios and (b) average BSOA over average OA concentration ratios, near surface, 4 August to 28 September 2006, HR6 sensitivity run.

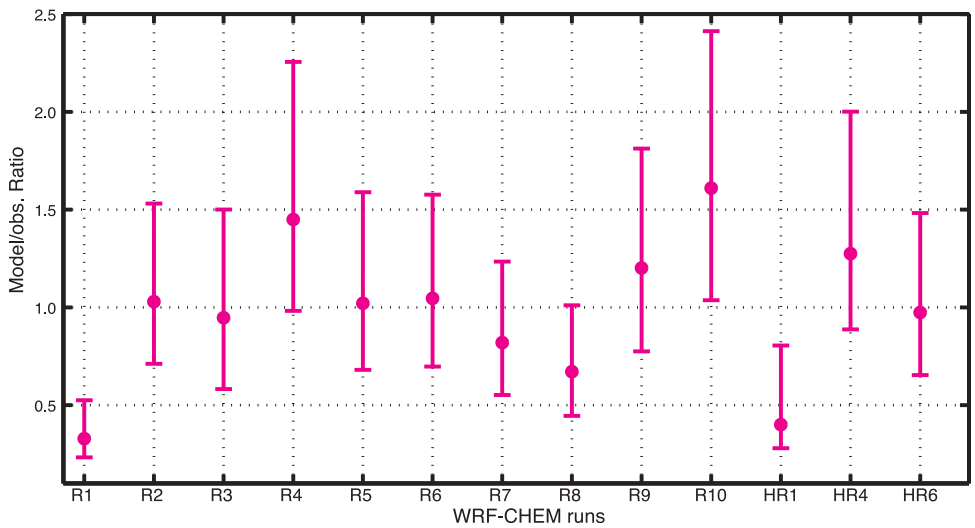

Figure 10. The model-aircraft bias statistics for OA measurements at 400–670 m altitude range during TexAQS-2006 campaign, over east Texas. The 25%, 50%, and 75% of the model-observation ratios for each model case are shown. For the R* and HR* runs 1978 and 2415 points from the model grids are used, respectively. The median of the observations is 3.68 μg/m^3.

especially at remote sites [*Schichtel et al.*, 2008]. *Schichtel et al.* [2008] reported decrease in modern carbon fraction toward northeastern United States and southeast of the Great Lakes compared to the other regions in the eastern United States during summer months. It should be noted that it is not straightforward to attribute the model anthropogenic POA to the fossil carbon solely, since the emission inventory used by our model contains POA from wood burning, cooking, waste treatment and so on. The same is true for EC as well.

3.3. Evaluation of OA Aloft: TexAQS-2006 Field Campaign

[55] In September 2006, the Texas Air Quality Study intensive field campaign took place in southeast Texas. During the campaign the NOAA P3 aircraft performed 10 daytime flights between 11 September and 29 September over Houston, Dallas and surrounding areas. The P3 aircraft sampled upwind and downwind areas of the cities, measuring a large variety of the atmospheric constituents including OA by AMS. The detailed description of the flights, meteorological conditions and OA measurements can be found in the work by *McKeen et al.* [2009] and *Bahreini et al.* [2009]. The AMS reports total nonrefractory OA mass, thus allowing a direct comparison to the modeled OA with the observations without assuming an OM:OC conversion factor. We compare all the WRF-CHEM runs with the OA measurements taken 400–670 m above the ground, which allows an evaluation of the SOA scheme's ability to characterize the enhancement of OA downwind of the strong urban sources. The aircraft is "flown" through the model grid and then measurements are averaged within each grid cell in order to compare against the model results. The results of this evaluation are given in Figure 10. Similar to the comparison for the surface sites, the R1 and HR1 runs underestimate OA by about 50%. Other runs (R7–R8) show less underestimation. The runs R4, R9, R10 and HR4 result in some overestimation. The median biases for five runs, R2, R3, R5, R6 and HR6 are very close to unity, while their lower and upper percentiles exhibit ±50% spread. The spread of the model error is a rough indication for overall correlation, and the runs with "good" median values tend to show less spread. The errors for the R4, R10 and HR4 model runs are skewed toward overestimation. It should be emphasized that the model's ability to simulate the aircraft measurements also depends strongly on its skill to capture the direction and width of urban plumes. Certainly this is very hard to achieve given the model's resolution of 60 or 20 km. Future model studies with higher spatial resolution should be performed to analyze these aircraft flights individually in more detail.

4. Conclusions

[56] Inclusion of the VBS formulation for SOA production, updated SOA yields, and multigenerational VOC oxidation within the WRF-CHEM model results in a significant improvement of the OA predictions compared to its standard version. The implementation of the new SOA scheme within the MADE aerosol module makes it possible to apply the WRF-CHEM model for air quality applications requiring better OA predictions with reasonable computational cost. The code will be available to the modeling community via the upcoming official release of the WRF-CHEM model (http://www.wrf-model.org). Given the broad user community of the WRF-CHEM model the new SOA scheme could be tested in different regions.

[57] The SOA model evaluations are complicated by uncertainties in the meteorology, anthropogenic and biogenic emissions, atmospheric oxidation, and removal processes. Thirteen model test runs are used to address some of the major uncertainties affecting the SOA simulations, and several major conclusions result from our evaluations. Primarily, it is clear that using recently reported traditional SOA yields still significantly underestimate observed OA concentrations without the inclusion of the OCV aging mechanism or so-called multigenerational oxidation of VOCs. The modeled POA

simulations alone exhibit less correlation compared to the measured OC, indicating the model's capability in capturing the spatiotemporal variability in the OC fields requires reasonable SOA simulations. The combination of the biogenic VOC emissions, their reported SOA yields, and the biogenic OCV aging result in biogenic SOA being the dominant OA component for much of the nonurban United States. Also, the diurnal cycle of OC at the southeastern SEARCH sites is mainly driven by biogenic SOA.

[58] Our sensitivity analysis has shown that the PBL scheme alters the results somewhat (≈10%), suggesting that there is a noticeable uncertainty in OC simulations due to the meteorological simulations. The model resolution does not affect the results very much. It should be noted that in some cases, such as simulating urban plumes or sites located in complex terrain or near the coast, higher spatial resolution may be necessary. We have found the positive impact of increasing resolution on simulating EC, especially the hourly concentrations. However, we do not see a clear improvement in hourly and daily OA simulations across the networks in higher-resolution cases. Future modeling studies in high resolution are required targeting individual measurement sites.

[59] On average the modeled POA comprise ≈10–20% (in carbon mass) of the measured OC concentrations at the urban and remote sites. The fraction of POA for the IMPROVE may be overestimated due to the possible underestimation of OC by the measurements [*Malm et al.*, 2011]. It should be noted that there are some uncertainties in the POA emissions as well. There is a discussion in the literature about overestimation of POA emissions in the anthropogenic inventories [*de Gouw and Jimenez*, 2009], and some part of the POA may be required to be treated as semivolatile in the models [*Robinson et al.*, 2007].

[60] Other uncertainties in the underlying SOA mechanism basically may be divided in two categories, SOA formation pathways, and removal processes. For instance, the SOA yields are very NO_x sensitive for some species such as aromatics, isoprene and monoterpenes (Table 4). The large range of SOA yields imposes another constraint on model performance. Our simulations that include the aging mechanism show that a reduced SOA yields may give similar results as default yields with a higher dry deposition of OCVs.

[61] Another key uncertainty in SOA formation is the aging mechanism. It is uncertain how much aging takes place after the first generation SOA product is formed and whether reverse process, fragmentation, may occur. Second, an important question is how aging is different for anthropogenic and biogenic OCVs. Some authors consider aging of anthropogenic OCVs only as a more realistic approach, since they report large overestimation of SOA in southeast United States when the biogenic OCVs are also aged [*Murphy and Pandis*, 2009, 2010]. From our study it becomes clear that the aging of both anthropogenic and biogenic OCVs result in a good agreement with the observations, with an adjustable bias that depends on the assumed dry deposition rate of the OCVs or aging rate. The model comparisons of OA with the aircraft AMS measurements show similar results as the surface network. Assuming both anthropogenic and biogenic OCVs are aged with an OH reaction rate of 1×10^{-11} cm^3 molec^{-1} s^{-1}, our evaluations for both surface and aircraft observations yield a recommended optimum value for the dry deposition rate of OCVs to be in a range of 0.25–0.5 that of HNO_3. This recommendation may change when reliable wet deposition and aqueous phase SOA parameterizations are included in the model.

[62] In addition the aging mechanism has an implication for fraction of ASOA and BSOA in OA. The radiocarbon analysis indicates significant modern carbon in ambient OA [*Hoyle et al.*, 2011; *Schichtel et al.*, 2008]. Our simulations (Figures 2 and 9b) show only multigenerational oxidation of biogenic VOCs may result in BSOA fractions comprising half or more OA mass. Undoubtedly the aging mechanism could be improved in future by involving more laboratory and field measurements.

[63] Our results suggest that the dry deposition of OCVs could have a significant impact on the SOA concentrations. Moreover, the dry deposition is an inevitable removal process within the boundary layer affecting the SOA concentrations in all the cases. As *Farina et al.* [2010] showed the wet deposition of OCVs can also play an important role in determining the SOA budget in the atmosphere. However, this removal mechanism is highly sensitive to the Henry's law constant assumed for the OCVs in their model. The inclusion of cloud phase processes for SOA has some implications. First of all this would reduce atmospheric SOA concentrations by wet deposition, but on the other hand the aqueous phase chemistry could be another significant SOA formation source [*Ervens et al.*, 2008; *Fu et al.*, 2009], which is not included in our model. We think that unlike dry deposition the role of wet deposition is possible to minimize when precipitation does not occur, for example in the case of the TexAQS-2006 flights (Figure 10), which were performed during periods without precipitation. Nevertheless the wet removal and aqueous phase SOA formation processes should be addressed in future model studies of relevant field experiments.

[64] Observations are indispensable in the model evaluation, especially the long-term ones. However, as our comparisons show, the daily averaged OC concentrations have some limitations in the model evaluations. As the time series from the SEARCH network show the highest OC concentrations occur during nighttime or early morning. Due to the difficulties in simulating the nocturnal shallow PBL, the models may have a strong bias in simulating the high nighttime OC concentrations, and consequently the model biases for daily averages could be mistakenly attributed to the SOA mechanism rather than vertical mixing. The results suggest that using hourly or at least daytime averaged OC measurements reported from different regions would be more beneficial rather than the daily averages for model evaluation and analysis of data.

[65] Uncertainties and inconsistencies between different OC and EC measurement techniques and standards [*Chow et al.*, 2010] also complicate the model evaluations. For example the median of the OC observations for the same time period and region for the STN network (after blank correction) data is 2.27 times higher than for the IMPROVE network (Table 6). Due to this large difference in the observed OC concentrations, we find that most of the model

runs with aging demonstrate significant overestimation for the IMPROVE network comparisons, but not for the STN, SEARCH and the aircraft comparisons. As noted earlier the possible underestimation of OC at the IMPROVE sites [*Malm et al.*, 2011] may partially explain this discrepancy between the networks. A model overestimation for IMPROVE and underestimation for the STN sites have been reported in other studies as well [e.g., *Murphy and Pandis*, 2009].

[66] The AMS measurements are advantageous since they measure total OA mass with high frequency, which makes the model-observation comparison for OA easy without the need to assume OM:OC ratios. However, the overall AMS data coverage is very limited in time and space, and OA measurements have an uncertainty of ≈38% [*Bahreini et al.*, 2009; *Middlebrook et al.*, 2012].

[67] One may conclude that the SOA models with recently proposed VBS-based formalisms solve the persistent underestimation problem of several regional-scale air quality models including WRF-CHEM. However, several related questions arise: how to prove or disprove these mechanisms, and how to determine key parameters driving SOA formation and removal processes using available or future measurements. Our study concludes that total OC concentrations may not be sufficient to address these questions even when aircraft OA data or hourly OC measurements are used.

[68] Consequently, future studies should focus on regions and time periods where information on meteorological variables, different types of OA, their surface fluxes, as well as advanced chemical measurements are available from intensive field campaigns. Studies combining high-resolution WRF-CHEM modeling with proposed SOA mechanisms will allow us to address some uncertainties outlined here and by other authors. Such modeling approaches can reduce existing uncertainties by treating additional OA characteristics, such as its oxidation state, which is possible by extending the current SOA modeling framework to a 2-D VBS as outlined by *Jimenez et al.* [2009] and [*Donahue et al.*, 2011].

[69] **Acknowledgments.** This work is funded by the NOAA United States Weather Research Program through the NOAA Office of Atmospheric Research. We are grateful to G. Grell, S. Peckham, and S.W. Kim for their support in development and running of the WRF-CHEM model. The authors also thank D. Murphy and J. Jimenez for productive discussions. The authors are grateful to the sponsors and administrators of the IMPROVE and STN networks for providing long-term aerosol composition measurements.

References

Ackermann, I. J., H. Hass, M. Memmesheimer, A. Ebel, F. S. Binkowski, and U. Shankar (1998), Modal aerosol dynamics model for Europe: Development and first applications, *Atmos. Environ.*, *32*(17), 2981–2999, doi:10.1016/S1352-2310(98)00006-5.

Bahreini, R., et al. (2009), Organic aerosol formation in urban and industrial plumes near Houston and Dallas, Texas, *J. Geophys. Res.*, *114*, D00F16, doi:10.1029/2008JD011493.

Bessagnet, B., C. Seigneur, and L. Menut (2010), Impact of dry deposition of semi-volatile organic compounds on secondary organic aerosols, *Atmos. Environ.*, *44*(14), 1781–1787, doi:10.1016/j.atmosenv.2010.01.027.

Bhave, P. V., G. A. Pouliot, and M. Zheng (2007), Diagnostic model evaluation for carbonaceous $PM_{2.5}$ using organic markers measured in the southeastern U.S., *Environ. Sci. Technol.*, *41*(5), 1577–1583, doi:10.1021/es061785x.

Carlton, A. G., C. Wiedinmyer, and J. H. Kroll (2009), A review of secondary organic aerosol (SOA) formation from isoprene, *Atmos. Chem. Phys.*, *9*(14), 4987–5005, doi:10.5194/acp-9-4987-2009.

Carlton, A. G., P. V. Bhave, S. L. Napelenok, E. D. Edney, G. Sarwar, R. W. Pinder, G. A. Pouliot, and M. Houyoux (2010), Model representation of secondary organic aerosol in CMAQv4.7, *Environ. Sci. Technol.*, *44*(22), 8553–8560, doi:10.1021/es100636q.

Chan, A. W. H., M. M. Galloway, A. J. Kwan, P. S. Chhabra, F. N. Keutsch, P. O. Wennberg, R. C. Flagan, and J. H. Seinfeld (2009), Photooxidation of 2-methyl-3-buten-2-ol as a potential source of secondary organic aerosol, *Environ. Sci. Technol.*, *43*(21), 8470, doi:10.1021/es902789a.

Chow, J. C., J. G. Watson, L. W. A. Chen, J. Rice, and N. H. Frank (2010), Quantification of $PM_{2.5}$ organic carbon sampling artifacts in US networks, *Atmos. Chem. Phys.*, *10*(12), 5223–5239, doi:10.5194/acp-10-5223-2010.

de Gouw, J., and J. L. Jimenez (2009), Organic aerosols in the Earth's atmosphere, *Environ. Sci. Technol.*, *43*(20), 7614–7618, doi:10.1021/es9006004.

de Gouw, J. A., et al. (2008), Sources of particulate matter in the northeastern United States in summer: 1. Direct emissions and secondary formation of organic matter in urban plumes, *J. Geophys. Res.*, *113*, D08301, doi:10.1029/2007JD009243.

de Gouw, J. A., C. Warneke, S. A. Montzka, J. S. Holloway, D. D. Parrish, F. C. Fehsenfeld, E. L. Atlas, R. J. Weber, and F. M. Flocke (2009), Carbonyl sulfide as an inverse tracer for biogenic organic carbon in gas and aerosol phases, *Geophys. Res. Lett.*, *36*, L05804, doi:10.1029/2008GL036910.

Donahue, N. M., A. L. Robinson, C. O. Stanier, and S. N. Pandis (2006), Coupled partitioning, dilution, and chemical aging of semivolatile organics, *Environ. Sci. Technol.*, *40*(8), 2635–2643, doi:10.1021/es052297c.

Donahue, N. M., S. A. Epstein, S. N. Pandis, and A. L. Robinson (2011), A two-dimensional volatility basis set: 1. Organic-aerosol mixing thermodynamics, *Atmos. Chem. Phys.*, *11*(7), 3303–3318, doi:10.5194/acp-11-3303-2011.

Erisman, J. W., A. Vanpul, and P. Wyers (1994), Parametrization of surface-resistance for the quantification of atmospheric deposition of acidifying pollutants and ozone, *Atmos. Environ.*, *28*(16), 2595–2607, doi:10.1016/1352-2310(94)90433-2.

Ervens, B., A. G. Carlton, B. J. Turpin, K. E. Altieri, S. M. Kreidenweis, and G. Feingold (2008), Secondary organic aerosol yields from cloud-processing of isoprene oxidation products, *Geophys. Res. Lett.*, *35*, L02816, doi:10.1029/2007GL031828.

Farina, S. C., P. J. Adams, and S. N. Pandis (2010), Modeling global secondary organic aerosol formation and processing with the volatility basis set: Implications for anthropogenic secondary organic aerosol, *J. Geophys. Res.*, *115*, D09202, doi:10.1029/2009JD013046.

Fu, T. M., D. J. Jacob, and C. L. Heald (2009), Aqueous-phase reactive uptake of dicarbonyls as a source of organic aerosol over eastern North America, *Atmos. Environ.*, *43*(10), 1814–1822, doi:10.1016/j.atmosenv.2008.12.029.

Goldstein, A. H., C. D. Koven, C. L. Heald, and I. Y. Fung (2009), Biogenic carbon and anthropogenic pollutants combine to form a cooling haze over the southeastern United States, *Proc. Natl. Acad. Sci. U. S. A.*, *106*(22), 8835–8840, doi:10.1073/pnas.0904128106.

Grell, G. A., S. E. Peckham, R. Schmitz, S. A. McKeen, G. Frost, W. C. Skamarock, and B. Eder (2005), Fully coupled "online" chemistry within the WRF model, *Atmos. Environ.*, *39*(37), 6957–6975, doi:10.1016/j.atmosenv.2005.04.027.

Hallquist, M., et al. (2009), The formation, properties and impact of secondary organic aerosol: Current and emerging issues, *Atmos. Chem. Phys.*, *9*(14), 5155–5236, doi:10.5194/acp-9-5155-2009.

Hansen, D. A., E. S. Edgerton, B. E. Hartsell, J. J. Jansen, N. Kandasamy, G. M. Hidy, and C. L. Blanchard (2003), The southeastern aerosol research and characterization study: Part 1—Overview, *J. Air Waste Manage. Assoc.*, *53*, 1460–1471.

Hansen, D. A., et al. (2006), Air quality measurements for the aerosol research and inhalation epidemiology study, *J. Air Waste Manage. Assoc.*, *56*, 1445–1458.

Heald, C. L., D. J. Jacob, R. J. Park, L. M. Russell, B. J. Huebert, J. H. Seinfeld, H. Liao, and R. J. Weber (2005), A large organic aerosol source in the free troposphere missing from current models, *Geophys. Res. Lett.*, *32*, L18809, doi:10.1029/2005GL023831.

Hildebrandt, L., N. M. Donahue, and S. N. Pandis (2009), High formation of secondary organic aerosol from the photo-oxidation of toluene, *Atmos. Chem. Phys.*, *9*(9), 2973–2986, doi:10.5194/acp-9-2973-2009.

Hildebrandt, L., K. M. Henry, J. H. Kroll, D. R. Worsnop, S. N. Pandis, and N. M. Donahue (2011), Evaluating the mixing of organic aerosol components using high-resolution aerosol mass spectrometry, *Environ. Sci. Technol.*, *45*(15), 6329–6335, doi:10.1021/es200825g.

Hodzic, A., J. L. Jimenez, S. Madronich, M. R. Canagaratna, P. F. DeCarlo, L. Kleinman, and J. Fast (2010), Modeling organic aerosols in a megacity: Potential contribution of semi-volatile and intermediate volatility

primary organic compounds to secondary organic aerosol formation, *Atmos. Chem. Phys.*, *10*(12), 5491–5514, doi:10.5194/acp-10-5491-2010.

Hoyle, C. R., et al. (2011), A review of the anthropogenic influence on biogenic secondary organic aerosol, *Atmos. Chem. Phys.*, *11*(1), 321–343, doi:10.5194/acp-11-321-2011.

Jimenez, J. L., et al. (2009), Evolution of organic aerosols in the atmosphere, *Science*, *326*(5959), 1525–1529, doi:10.1126/science.1180353.

Kleindienst, T. E., M. Jaoui, M. Lewandowski, J. H. Offenberg, C. W. Lewis, P. V. Bhave, and E. O. Edney (2007), Estimates of the contributions of biogenic and anthropogenic hydrocarbons to secondary organic aerosol at a southeastern US location, *Atmos. Environ.*, *41*(37), 8288–8300, doi:10.1016/j.atmosenv.2007.06.045.

Kroll, J. H., A. W. H. Chan, N. L. Ng, R. C. Flagan, and J. H. Seinfeld (2007), Reactions of semivolatile organics and their effects on secondary organic aerosol formation, *Environ. Sci. Technol.*, *41*(10), 3545–3550, doi:10.1021/es062059x.

Lane, T. E., N. M. Donahue, and S. N. Pandis (2008a), Simulating secondary organic aerosol formation using the volatility basis-set approach in a chemical transport model, *Atmos. Environ.*, *42*(32), 7439–7451, doi:10.1016/j.atmosenv.2008.06.026.

Lane, T. E., N. M. Donahue, and S. N. Pandis (2008b), Effect of NOx on secondary organic aerosol concentrations, *Environ. Sci. Technol.*, *42*(16), 6022–6027, doi:10.1021/es703225a.

Malm, W. C., B. A. Schichtel, and M. L. Pitchford (2011), Uncertainties in $PM_{2.5}$ gravimetric and speciation measurements and what we can learn from them, *J. Air Waste Manage. Assoc.*, *61*, 1131–1149.

McKeen, S., et al. (2007), Evaluation of several $PM_{2.5}$ forecast models using data collected during the ICARTT/NEAQS 2004 field study, *J. Geophys. Res.*, *112*, D10S20, doi:10.1029/2006JD007608.

McKeen, S., et al. (2009), An evaluation of real-time air quality forecasts and their urban emissions over eastern Texas during the summer of 2006 Second Texas Air Quality Study field study, *J. Geophys. Res.*, *114*, D00F11, doi:10.1029/2008JD011697.

Mellor, G. L., and T. Yamada (1982), Development of a turbulence closure-model for geophysical fluid problems, *Rev. Geophys.*, *20*(4), 851–875, doi:10.1029/RG020i004p00851.

Middlebrook, A. M., R. Bahreini, J. L. Jimenez, and M. R. Canagaratna (2012), Evaluation of composition-dependent collection efficiencies for the Aerodyne aerosol mass spectrometer using field data, *Aerosol Sci. Technol.*, *46*, 258–271.

Murphy, B. N., and S. N. Pandis (2009), Simulating the formation of semivolatile primary and secondary organic aerosol in a regional chemical transport model, *Environ. Sci. Technol.*, *43*(13), 4722–4728, doi:10.1021/es803168a.

Murphy, B. N., and S. N. Pandis (2010), Exploring summertime organic aerosol formation in the eastern United States using a regional-scale budget approach and ambient measurements, *J. Geophys. Res.*, *115*, D24216, doi:10.1029/2010JD014418.

Murphy, D. M., S. L. Capps, J. S. Daniel, G. J. Frost, and W. H. White (2008), Weekly patterns of aerosol in the United States, *Atmos. Chem. Phys.*, *8*(10), 2729–2739, doi:10.5194/acp-8-2729-2008.

Ng, N. L., J. H. Kroll, M. D. Keywood, R. Bahreini, V. Varutbangkul, R. C. Flagan, J. H. Seinfeld, A. Lee, and A. H. Goldstein (2006), Contribution of first-versus second-generation products to secondary organic aerosols formed in the oxidation of biogenic hydrocarbons, *Environ. Sci. Technol.*, *40*(7), 2283–2297, doi:10.1021/es052269u.

Ng, N. L., J. H. Kroll, A. W. H. Chan, P. S. Chhabra, R. C. Flagan, and J. H. Seinfeld (2007), Secondary organic aerosol formation from m-xylene, toluene, and benzene, *Atmos. Chem. Phys.*, *7*(14), 3909–3922, doi:10.5194/acp-7-3909-2007.

Odum, J. R., T. Hoffmann, F. Bowman, D. Collins, R. C. Flagan, and J. H. Seinfeld (1996), Gas/particle partitioning and secondary organic aerosol yields, *Environ. Sci. Technol.*, *30*(8), 2580–2585, doi:10.1021/es950943+.

Pankow, J. F. (1994), An absorption-model of the gas aerosol partitioning involved in the formation of secondary organic aerosol, *Atmos. Environ.*, *28*(2), 189–193, doi:10.1016/1352-2310(94)90094-9.

Papiez, M. R., M. J. Potosnak, W. S. Goliff, A. B. Guenther, S. N. Matsunaga, and W. R. Stockwell (2009), The impacts of reactive terpene emissions from plants on air quality in Las Vegas, Nevada, *Atmos. Environ.*, *43*(27), 4109–4123, doi:10.1016/j.atmosenv.2009.05.048.

Pye, H. O. T., and J. H. Seinfeld (2010), A global perspective on aerosol from low-volatility organic compounds, *Atmos. Chem. Phys.*, *10*(9), 4377–4401, doi:10.5194/acp-10-4377-2010.

Robinson, A. L., N. M. Donahue, M. K. Shrivastava, E. A. Weitkamp, A. M. Sage, A. P. Grieshop, T. E. Lane, J. R. Pierce, and S. N. Pandis (2007), Rethinking organic aerosols: Semivolatile emissions and photochemical aging, *Science*, *315*(5816), 1259–1262, doi:10.1126/science. 1133061.

Schell, B., I. J. Ackermann, H. Hass, F. S. Binkowski, and A. Ebel (2001), Modeling the formation of secondary organic aerosol within a comprehensive air quality model system, *J. Geophys. Res.*, *106*(D22), 28,275–28,293, doi:10.1029/2001JD000384.

Schichtel, B. A., W. C. Malm, G. Bench, S. Fallon, C. E. McDade, J. C. Chow, and J. G. Watson (2008), Fossil and contemporary fine particulate carbon fractions at 12 rural and urban sites in the United States, *J. Geophys. Res.*, *113*, D02311, doi:10.1029/2007JD008605.

Schwede, D., G. Pouliot, and T. Pierce (2005), Changes to the biogenic emissions inventory system version 3 (BEIS3), paper presented at 4th Annual CMAS Model-3 User's Conference, Chapel Hill, N. C., 26–28 Sept.

Shrivastava, M., J. Fast, R. Easter, W. I. Gustafson Jr., R. A. Zaveri, J. L. Jimenez, P. Saide, and A. Hodzic (2011), Modeling organic aerosols in a megacity: Comparison of simple and complex representations of the volatility basis set approach, *Atmos. Chem. Phys.*, *11*(13), 6639–6662, doi:10.5194/acp-11-6639-2011.

Simon, H., P. V. Bhave, J. L. Swall, N. H. Frank, and W. C. Malm (2011), Determining the spatial and seasonal variability in OM/OC ratios across the US using multiple regression, *Atmos. Chem. Phys.*, *11*(6), 2933–2949, doi:10.5194/acp-11-2933-2011.

Spracklen, D. V., J. A. Logan, L. J. Mickley, R. J. Park, R. Yevich, A. L. Westerling, and D. A. Jaffe (2007), Wildfires drive interannual variability of organic carbon aerosol in the western U.S. in summer, *Geophys. Res. Lett.*, *34*, L16816, doi:10.1029/2007GL030037.

Stockwell, W. R., F. Kirchner, M. Kuhn, and S. Seefeld (1997), A new mechanism for regional atmospheric chemistry modeling, *J. Geophys. Res.*, *102*(D22), 25,847–25,879, doi:10.1029/97JD00849.

Stroud, C. A., et al. (2011), Impact of model grid spacing on regional- and urban-scale air quality predictions of organic aerosol, *Atmos. Chem. Phys.*, *11*(7), 3107–3118, doi:10.5194/acp-11-3107-2011.

Tsimpidi, A. P., V. A. Karydis, M. Zavala, W. Lei, L. Molina, I. M. Ulbrich, J. L. Jimenez, and S. N. Pandis (2010), Evaluation of the volatility basis-set approach for the simulation of organic aerosol formation in the Mexico City metropolitan area, *Atmos. Chem. Phys.*, *10*(2), 525–546, doi:10.5194/acp-10-525-2010.

U.S. Environmental Protection Agency (2010), EPA clearing-house for inventories and emissions factors: 2005 National Emission Inventory documentation and data—Final version 3.0, report, Washington, D. C. [Available at http://www.epa.gov/ttn/chief/net/2005inventory.html.]

Volkamer, R., J. L. Jimenez, F. San Martini, K. Dzepina, Q. Zhang, D. Salcedo, L. T. Molina, D. R. Worsnop, and M. J. Molina (2006), Secondary organic aerosol formation from anthropogenic air pollution: Rapid and higher than expected, *Geophys. Res. Lett.*, *33*, L17811, doi:10.1029/2006GL026899.

Weber, R. J., et al. (2007), A study of secondary organic aerosol formation in the anthropogenic-influenced southeastern United States, *J. Geophys. Res.*, *112*, D13302, doi:10.1029/2007JD008408.

Wesely, M. L., and B. B. Hicks (2000), A review of the current status of knowledge on dry deposition, *Atmos. Environ.*, *34*(12–14), 2261–2282, doi:10.1016/S1352-2310(99)00467-7.

Yu, S., P. V. Bhave, R. L. Dennis, and R. Mathur (2007), Seasonal and regional variations of primary and secondary organic aerosols over the continental United States: Semi-empirical estimates and model evaluation, *Environ. Sci. Technol.*, *41*(13), 4690–4697, doi:10.1021/es061535g.

Zhang, Q., D. R. Worsnop, M. R. Canagaratna, and J. L. Jimenez (2005), Hydrocarbon-like and oxygenated organic aerosols in Pittsburgh: Insights into sources and processes of organic aerosols, *Atmos. Chem. Phys.*, *5*(12), 3289–3311, doi:10.5194/acp-5-3289-2005.

Zhang, Q., et al. (2007), Ubiquity and dominance of oxygenated species in organic aerosols in anthropogenically-influenced Northern Hemisphere midlatitudes, *Geophys. Res. Lett.*, *34*, L13801, doi:10.1029/2007GL029979.

R. Ahmadov, R. Bahreini, J. A. de Gouw, E.-Y. Hsie, S. A. McKeen, J. Meagher, A. M. Middlebrook, and M. Trainer, Chemical Sciences Division, Earth System Research Laboratory, NOAA, 325 Broadway, Boulder, CO 80305, USA. (ravan.ahmadov@noaa.gov)

E. Edgerton, Atmospheric Research and Analysis, Inc., Cary, NC 27513, USA.

A. L. Robinson, Center for Atmospheric Particle Studies, Carnegie Mellon University, Pittsburgh, PA 15213, USA.

S. Shaw, Electric Power Research Institute, 3420 Hillview Ave., Palo Alto, CA 94304, USA.